

CHANGE DETECTION OF *TAMARIX SPP.* IN  
THE UPPER BRAZOS RIVER CORRIDOR  
USING OBJECT-BASED  
IMAGE ANALYSIS

by

Tighearnan G. Juarez Murphy, B.S.

A thesis submitted to the Graduate Council of  
Texas State University in partial fulfillment  
of the requirements for the degree of  
Master of Science  
with a Major in Geography  
August 2022

Committee Members:

Kimberly Meitzen, Chair

Samantha Krause

Nathan Currit

**COPYRIGHT**

by

Tighearnan G. Juarez Murphy

2022

## **FAIR USE AND AUTHOR'S PERMISSION STATEMENT**

### **Fair Use**

This work is protected by the Copyright Laws of the United States (Public Law 94-553, section 107). Consistent with fair use as defined in the Copyright Laws, brief quotations from this material are allowed with proper acknowledgement. Use of this material for financial gain without the author's express written permission is not allowed.

### **Duplication Permission**

As the copyright holder of this work I, Tighearnan G. Juarez Murphy, authorize duplication of this work, in whole or in part, for educational or scholarly purposes only.

## **DEDICATION**

I dedicate this thesis to the two Lindsays in my life.



## **ACKNOWLEDGEMENTS**

Many thanks go to my advisor Dr. Kimberly Meitzen for all your support and guidance.

Thank you for your time to help guide me through this process. Also, thank you for showing me that quicksand is real, and it can get pretty deep. I want to thank Dr. Samantha Krause for giving me invaluable resources and opportunities to hone my field skills, and for your always positive attitude even after a long and hot day. I would also like to thank Dr. Nathan Currit for giving me the tools necessary to expand my knowledge in an area I had very little knowledge about and sparking a yearning to know more. A big thank you also goes to Izzy and Aspen for your hard work in the field and helping me get vegetation points. Finally, I want to thank my wife, Lindsay. Beyond your homecooked meals you sent with me into the field, your never wavering support is what has brought me to this point.

## TABLE OF CONTENTS

	Page
ACKNOWLEDGEMENTS.....	v
LIST OF TABLES .....	viii
LIST OF FIGURES .....	x
LIST OF ABBREVIATIONS .....	xi
ABSTRACT .....	xiii
 CHAPTER	
I. INTRODUCTION.....	1
Background .....	1
Problem Statement .....	2
Justification .....	4
Objectives .....	5
II. LITERATURE REVIEW.....	6
History of <i>Tamarix spp.</i> and Introduction to North America .....	6
<i>Tamarix spp.</i> in Texas .....	7
<i>Tamarix spp.</i> as an Exotic and Invasive Species .....	9
Management Techniques in Texas .....	15
Remote Sensing of <i>Tamarix spp.</i> .....	18
Utilization of OBIA for Mapping Riparian Vegetation .....	18
III. METHODOLOGY .....	21
Study Area .....	21
Data Collection .....	26
Data Preprocessing .....	27
Object-Based Image Classification .....	29
Accuracy Assessment .....	33
Stratified Image Approach.....	36
Change Detection .....	36

IV. RESULTS .....	38
Image Classification .....	38
Accuracy Assessments .....	49
Change Detection .....	58
V. DISCUSSION .....	67
NAIP Imagery .....	67
Field Data Collection .....	68
Image Classification .....	69
Accuracy Assessment.....	70
Change Detection .....	70
Next Steps .....	71
VI. CONCLUSION .....	73
REFERENCES .....	75

## LIST OF TABLES

<b>Table</b>	<b>Page</b>
1. Collection dates for NAIP imagery in 2012 and 2020 .....	26
2. Segmentation parameters for NFD MF 1 and NFD MF 1 floodplain .....	29
3. Segmentation parameters for NFD MF 2 .....	30
4. Segmentation parameters for DMF 0 .....	30
5. Class categories and values for NFD MF 1 and NFD MF 1 floodplain .....	31
6. Class categories and values for NFD MF 2 .....	31
7. Class categories and values for DMF 0 .....	31
8. Random Forest image classification parameters .....	33
9. Minimum number of sample points required for accuracy assessment using MDE.....	35
10. Class counts and percentages for NFD MF 1 2012 .....	38
11. Class counts and percentages for NFD MF 1 2020 .....	38
12. Class counts and percentages for NFD MF 2 2012 .....	38
13. Class counts and percentages for NFD MF 2 2020 .....	39
14. Class counts and percentages for DMF 0 2012 .....	39
15. Class counts and percentages for DMF 0 2020 .....	39
16. Class counts and percentages for NFD MF 1 2012 floodplain.....	39
17. Class counts and percentages for NFD MF 1 2020 floodplain.....	40
18. Accuracy assessment for classified NFD MF 1 2012 .....	50
19. Accuracy assessment for classified NFD MF 1 2020 .....	51

20. Accuracy assessment for classified NFDMF 2 2012 .....	52
21. Accuracy assessment for classified NFDMF 2 2020 .....	53
22. Accuracy assessment for classified DMF 0 2012.....	54
23. Accuracy assessment for classified DMF 0 2020.....	55
24. Accuracy assessment for classified NFDMF 1 2012 floodplain.....	56
25. Accuracy assessment for classified NFDMF 1 2020 floodplain.....	57
26. Changed pixels and percent change of saltcedar .....	58

## LIST OF FIGURES

Figure	Page
1. NAIP image of NFD MF 1 .....	23
2. NAIP image of NFD MF 2 .....	24
3. NAIP image of DMF 0.....	25
4. Classified map of NFD MF 1 2012 .....	41
5. Classified map of NFD MF 1 2020 .....	42
6. Classified map of NFD MF 2 2012 .....	43
7. Classified map of NFD MF 2 2020 .....	44
8. Classified map of DMF 0 2012 .....	45
9. Classified map of DMF 0 2020 .....	46
10. Classified map of NFD MF 1 2012 floodplain .....	47
11. Classified map of NFD MF 1 2020 floodplain .....	48
12. Change detection of saltcedar for NFD MF 1 .....	59
13. Change detection of unchanged saltcedar for NFD MF 1 .....	60
14. Change detection of saltcedar for NFD MF 2 .....	61
15. Change detection of unchanged saltcedar for NFD MF 2 .....	62
16. Change detection of saltcedar for DMF 0 .....	63
17. Change detection of unchanged saltcedar for DMF 0 .....	64
18. Change detection of saltcedar for NFD MF 1 floodplain .....	65
19. Change detection of unchanged saltcedar for NFD MF 1 floodplain.....	66

## LIST OF ABBREVIATIONS

Abbreviation	Description
AOI	Area of Interest
CIR	Color Infrared
DMF 0	Double Mountain Fork 0
DN	Digital Number
ENT	Entropy
ET	Evapotranspiration
GLCM	Grey Level Co-Occurrence Matrix
GPS	Global Positioning System
MDE	Multinomial Distribution Equation
NAD 83	North American Datum 1983
NAIP	National Agricultural Imagery Program
NDVI	Normalized Difference Vegetation Index
NDWI	Normalized Difference Water Index
NFDMF 1	North Fork Double Mountain Fork 1
NFDMF 2	North Fork Double Mountain Fork 2
NIR	Near Infrared
OBIA	Object-Based Image Analysis
RF	Random Forests
RGB	Red, Green, and Blue

SfM	Structure from Motion
TEAM	Texas Ecosystems Analytical Mapper
TNRIS	Texas Natural Resources Information Systems
ToA	Top-of-Atmosphere
TPWD	Texas Parks and Wildlife Department
UBR	Upper Brazos River
UTM	Universal Transverse Mercator



## ABSTRACT

Woody phreatophytes are some of the most impactful invasive species in the upper Brazos River (UBR), with saltcedar (*Tamarix spp.*) being of most concern. Since saltcedar's introduction to the eastern United States in the late 1800's, it quickly grew to become a nuisance. This invasive species alters instream sedimentation dynamics, channel and floodplain morphology, and riparian vegetation throughout the southwestern United States. The removal and eradication of this species is a multi-million dollar per year project. This thesis uses high-resolution imagery and object-based image classification methods to measure changes in saltcedar cover within the UBR relative to pre- and post-management efforts, over the period of 2017-2020, led by Texas Parks and Wildlife Department. During the study period, analysis revealed an overall decrease in saltcedar, indicating that management efforts have been effective in decreasing the amount of healthy saltcedar that occur in the UBR.

## I. INTRODUCTION

### Background

The Brazos River is the third longest river (1,352 km) in the state of Texas, the second largest river basin by area (119, 174 km<sup>2</sup>) and has the largest average annual discharge volume (237.5 m<sup>3</sup>/s) of all Texas rivers (Hendrickson, 2002). The Brazos River's water resources are vital to the state's economic activities such as crop agriculture, ranching, municipal, and industrial water supply. Historically, the Brazos River is second to only the Mississippi River in amount of sediment that is transported to the Gulf of Mexico at approximately ~ 10 – 16 metric tons per year (Milliman and Meade, 1983).

Saltcedar (*Tamarix spp.*) is a woody, shrub-like phreatophyte that originates from regions that include southern Europe, the eastern Mediterranean, and northern Africa, and was introduced into the U.S. (Baum, 1967). Saltcedar was the name given to these shrubs due to the small scale-like leaves that appear to resemble leaves of cedars, as well as the saline exudate that accumulates on the foliage (Fraiser and Johnsen, 1991). Once hailed as a cost-effective and accessible option for wind breaks, shade, and streambank stabilization, saltcedar quickly became an invasive species by as early as the 1920's (Botherson and Winkel, 1986). Since their introduction, saltcedar has invaded many ecosystems throughout the United States, with much of their concentrations found within the southwestern states spanning from California to north Texas and Oklahoma (Neill, 1985; Friederici, 1995). Their invasion has brought forth ecological and hydrological stresses that have required management efforts costing millions of dollars per year

(Zavaleta, 2000).

With the availability and accessibility of water becoming an issue of growing concern, especially in the American southwest, the management of invasive species like *Tamarix* has become a focal point of resource conservation (Seager et al., 2013; Elias et al., 2016; Miller et al., 2021). Saltcedar's roots reach and drain the water table adjacent to streams, altering local water budgets and increasing water losses. Much of the southwestern states are experiencing more frequent and intense droughts brought on by unsustainable practices and anthropogenic climate change (Diffenbaugh et al., 2015; Williams et al., 2020). These droughts have allowed *Tamarix* to expand their dominance due to their salinity tolerance (Gatewood et al., 1950; Carman and Brotherson, 1982; Brotherson and Winkel, 1986). This study will use high spatial resolution imagery to identify saltcedar coverage changes in high-density reaches within the upper Brazos River where management efforts have occurred since 2017.

## **Problem Statement**

Invasive species like *Tamarix* are altering the geometry, composition, and sedimentation of the upper Brazos River through sediment accumulation and channel narrowing (Nagler et al., 2008; Dean et al., 2011). Riparian banks stabilized by invasive saltcedar have the ability to transform shallow, wide, low-velocity braided streams into deeper and swifter flowing streams. These changes impact flood processes, native riparian communities, and instream aquatic habitats. Reduced water temperatures resulting from increased stream depth create colder conditions that directly impact warm-water adapted native fish. Previous studies have examined how invasive riparian

vegetation encroachment affects streams' responses to high flows, and how their removal can restore geomorphic dynamics of sediment remobilization. (Perignon et al., 2013; Vincent et al., 2009). Studies focusing on saltcedar influenced geomorphology within the UBR have not been conducted recently, with some of the most substantial research in the region conducted in the 1970's and 1980's (Busby and Schuster, 1973; Blackburn et al., 1982). The majority of recent studies on the fluvial geomorphology of the Brazos River focused on the middle and lower sections, with minimal emphasis on the influence of invasive riparian vegetation (Phillips, 2007; Taha and Anderson, 2008; Giardino and Lee, 2011).

Remote sensing of vegetation is an important methodological approach in the identification and management of invasive species, as managers require precise spatiotemporal information to assist their efforts of mitigation and eradication (Johnson, 1999). Traditional surveying methods including ground mapping utilizing instruments such as Global Positioning System (GPS) units result in high accuracies in small areas (Cooksey and Sheley, 1997). With management areas in the UBR usually exceeding thousands of hectares, this method of surveying may prove to be impractical for management efforts. Remote sensing of invasive vegetation species using high-resolution imagery is common (Glenn and Nagler, 2005; Akasheh et al., 2008; Huylenbroeck et al., 2020). Saltcedar identification has been conducted using both medium and high-resolution imagery (Wang et al., 2013; Ji and Wang, 2016). Methods have included object-based image analysis, phenological metrics, and indices such as Normalized Difference Vegetation Index (NDVI). Accurate spatial distribution mapping of saltcedar is imperative for proper systematic conservation of native species while removing the

invasive phreatophyte to restore these affected riparian ecosystems (Stromberg et al., 2009; Nagler et al., 2011). This research contains the spatial distribution of remotely sensed *Tamarix* in management areas. Images from 2012 and 2020 are used to calculate the change of saltcedar in these areas pre- and post-management.

## **Justification**

The results from this study will contribute to the management efforts of saltcedar, as well as provide recent data to examine the influence of riparian phreatophytes in the context of the UBR. This research could provide useful data to agencies such as Texas Parks and Wildlife Department (TPWD) whose aquatic invasive management efforts are some of the largest in the state.

TPWD is actively undertaking a large-scale collaborative management effort of *Tamarix* in north Texas. Beginning in 2016, partners including U.S. Fish and Wildlife Service (USFWS), and multiple Texas universities have aided TPWD in the targeted application of herbicides to manage the saltcedar invasion. Eradication activities have focused on tributaries of the upper Brazos River Basin, including the Salt Fork and North Fork Double Mountain Fork, as well as the main stem upstream of Possum Kingdom Lake (TPWD, 2018). Efforts also include the continued monitoring of riparian and instream habitats, as well as measurements to further assess how saltcedar affects local hydrology. This study will provide classified change detection maps of select reaches targeted by TPWD's removal efforts. Understanding the temporal and spatial responses of saltcedar vegetation changes will inform the monitoring and adaptive management efforts in the UBR. The techniques used in this study can be applied to examining

invasive phreatophytes in similar riparian corridors throughout the southwestern United States.

## **Objectives**

The goal of this research is to answer the research question: How has saltcedar presence, coverage, and distribution in riparian areas of the upper Brazos River Basin changed over the period of 2016 -2020? I will map saltcedar distribution in pre-defined management areas within the UBR via remotely sensed imagery and assess the change in vegetation cover linked to management efforts of the invasive species. TPWD is using targeted, aerial applications of herbicide on saltcedar to begin the restoration of riparian and instream habitats to support fish and wildlife, as well as healthy river function (TPWD, 2022). The images will be classified utilizing an Object-Based Image Analysis (OBIA) scheme to classify the images by land cover type, then a change detection will be calculated to quantify the change in saltcedar coverage. This relationship will highlight the effect of saltcedar management in repelling an invasive species while restoring river functionality. I will answer my research question using the following approach:

1. Acquire National Agricultural Imagery Program (NAIP) imagery of years 2012 and 2020 of pre-defined management areas.
2. Produce an object-based classification of NAIP imagery scenes.
3. Calculate change detection of saltcedar between image years and quantify changes in presence, coverage, and distribution.
4. Assess the effects of saltcedar management in selected areas and future implications.

## II. LITERATURE REVIEW

### **History of *Tamarix* spp. and Introduction to North America**

Within the native range of *Tamarix*, there are fifty four species that span from southern Europe, North Africa, the Middle East, India, Pakistan, and China (Baum, 1978). *Tamarix* has been found in fossilized charcoal records originating from Israel that date back to before 10,000 YBP (Ley-Yadum and Weinstein-Evron, 1994). Naming of the plant's genus Tamaricaceae is thought to have been sourced from either Tamaro River located in Nepal, or possibly the Tamaris River in Spain (Crins, 1989; DiTomaso, 1998). Currently, there are eight species of *Tamarix* found throughout the United States and five species with concentrations within the southwest (DiTomaso, 1996).

Many theories exist on the timing of saltcedar introduction to North America and the United States.. Early hypotheses included introduction via the Spaniards as they travelled from southern Europe to the arid and semiarid regions of Mexico during their exploration of the New World. If populations of saltcedar were indeed established in this manner, then it would be logical to believe that central Mexico and the arid American southwest would be the epicenter of distribution (Bowser, 1958). Analysis of texts written by a Spanish padre during the late 18<sup>th</sup> century suggested observations of *Tamarix*, although the term used might have been misinterpreted and instead detailed native vegetation (Martinez, 1937; Auerbach, 1943). Further support of this mislabeling includes the lack of observations made by Spanish explorers as they crossed American rivers such as the Green and Colorado, both of which presently contain dense stands of saltcedar (Christensen, 1962).

The first known intentional introduction of *Tamarix* into the United States was documented by nursery workers in the early 1800's (Robinson, 1965). Evidence for this introduction timeline includes the offering of *Tamarix* for sale in New York City for ornamental plantings by the Old American Nursery in 1823 (Horton, 1964). Commercial availability of *Tamarix* expanded throughout the early 1800's along the eastern seaboard. An annual report from the U.S. Department of Agriculture listed six species of *Tamarix* that were being grown in their Arboretum Grounds in Washington D.C. (Horton, 1964). From the dispersal of these plants for ornamental plantings, they soon began their gradual escape from cultivation. By the early 1900's, specific species of saltcedar were encountered along roadsides in the south with regularity (Small, 1903). Endorsements of the possible benefits of saltcedar aided their expansion, these included ornamental plantings in arid environments for their utility as windbreak, shade for stock animals, and even fuel. Through these uses, the number of planned and unplanned plantings grew (Thornber, 1916).

### ***Tamarix* spp. in Texas**

Saltcedar was first collected in Texas in 1877, and it was one of the first specimens collected for study outside of their introduced habitats (Robinson, 1965). This specimen was collected on Galveston Island and was noted as being naturalized to its invaded habitat. Saltcedar was first introduced in Texas to mitigate streambank erosion, following a similar practice in other states (Everitt, 1998). Much of the early concentrations of saltcedar were located in the Rio Grande and Pecos rivers, where some of the earliest documentations of *Tamarix* in the southwest occurred in the early 1900's.



(Eakin and Brown, 1939; Thompson, 1958). According to Robinson (1965), the largest area of saltcedar was located within the Pecos River Basin in New Mexico and Texas, covering an aerial extent of 275,000 acres. Most of the area was within the Texas border and cover density varied from five to one hundred percent

It is hypothesized that from there, saltcedar dispersed eastward in Texas along connected river networks, invading suitable habitats. Much of the saltcedar in the United States occurs west of the 100<sup>th</sup> meridian where annual rainfall drops below 45 cm yr<sup>-1</sup> and agriculture becomes dependent on irrigation (Zavaleta, 2000). The UBR spans a gradient along this meridian boundary and has documented saltcedar invasion. Saltcedar in the UBR likely proliferated from fragmented stands that occurred hundreds of meters away from the channel where native mesquite created a barrier. Flooding allowed saltcedar propagules to migrate and establish closer to the channel (Blackburn et al., 1982). Sedimentation dynamics along the Brazos have been altered due to saltcedar presence. In 1940, sparse saltcedar stands were located on average 93 meters away from the channel and within ten years the average distance was reduced to 19 meters (Busby and Schuster 1973). Dense saltcedar stands averaged 111 meters from the channel in 1940 and reduced to just 13 meters in 1969 (Busby and Schuster, 1973).

Following establishment, saltcedar and native phreatophytes occupied fifty seven percent of the UBR upstream of Possum Kingdom Lake, an increase of eighteen percent from 1969 through 1979 (Blackburn et al., 1982). In 1969, saltcedar alone attributed to thirty six percent of the observed riparian vegetation within the UBR (Busby and Schuster, 1973). As a phreatophyte with the ability to consume large quantities of water, saltcedar is estimated to use approximately 44,000 acre-feet of water annually within the

tributaries and main stem of the Brazos upstream from Possum Kingdom Lake (Busby and Schuster, 1973). Sediment accumulation and hydrologic alteration has profoundly affected the shape and morphology of the UBR. A pair of photograph analyses of aerial images captured between 1939 and 1973 revealed the changes in stream position coinciding with saltcedar's proliferation in the region. Both analyses displayed the selected stream reaches narrowing due to rapid sedimentation accumulations (Busby and Schuster, 1973; Blackburn et al., 1982).

Saltcedar and phreatophyte proliferation along the floodplain and channel facilitated the accumulation of 3 meters of sediment, reducing the width of the Brazos by approximately 90 meters in reaches upstream of Possum Kingdom Lake (Busby and Schuster, 1973). Similar studies across the west have yielded comparable results. The Gila River, Arizona, experienced rapid expansion of saltcedar and displacement of native cottonwood and *Baccharis* between 1914 and 1964. As a result, mobilized sediments upstream from unaffected reaches of the Gila accumulated in dense saltcedar stands, drastically reducing the width of the channel (Turner, 1974). As saltcedar now occupies over 500,000 acres in Texas, its effects on rivers and riparian habitats have created a major management issue that proves to be a daunting task heading into an uncertain future in terms of water usage and availability (DeLoach et al., 2009).

### ***Tamarix spp.* as an Exotic and Invasive Species**

Exotic and invasive plant species are those that are introduced outside of their native range, establish populations, naturalize within their environment, and then disperse outside of their introduction range, and are detrimental to their introduced environment

(Mooney and Drake, 1989; Parker et al., 1999; Mack et al., 2000; Tickner et al., 2001).

Highly prolific invasive species are credited with becoming one of the leading causes of biodiversity loss (Pimentel et al., 2005). Invasive species establishments are widely studied because they alter ecosystem function and structure (Crown et al., 2008).

Until the mid-twentieth century, saltcedar was positively viewed in the context of riparian ecosystems. Sediment accumulation brought on by the expansion saltcedar was seen as a stabilizer against erosion along lake and channel edges, and the species' ability to desalinize deep soil profiles through their salt secretion was considered desirable (Goldsmith and Smart, 1982). Although these initial alterations to their environments were welcomed, the negative effects of saltcedar expansion were soon realized. Continued expansion and outcompeting of native vegetation has contributed to saltcedar being the most dominant woody riparian species in the west (Dudley et al., 2000; Doody et al., 2011).

Saltcedar expansion occurred at a time where much of the riparian vegetation was concurrently altered by westward expansion during the 1800's and early 1900's. Native phreatophytes along streams were harvested or cleared for anthropogenic uses and created an opening for saltcedar to expand their range (Horton and Campbell, 1974). The destruction of native vegetation from water management plans that drastically altered natural flow regimes of the western and southwestern United States greatly aided saltcedar's proliferation (Engel-Wilson and Ohmart, 1978; Everitt, 1980; Shafroth et al., 1995). Streamflow alterations have increased average soil salinities, such that native vegetation cannot survive, enabling the more saline resistant saltcedar to benefit (Brotherson and Field 1987; Sala and Smith 1996).

Comparisons between streams with native riparian cover and those with saltcedar, indicate that flooding and erosion disproportionately impact stream reaches dominated by the invasive saltcedar. Sediment accumulation caused by the extensive and sturdy *Tamarix* root systems reduced stream's lateral mobility (Graf, 1978). The sediment accumulation creates a positive feedback loop; as the sandbars, riverbanks, and midstream islands continue to grow and streams become progressively narrower. Stream narrowing increases streamflow velocity and the potential for severe flood events (Eagan et al. 1993; Fraiser and Johnsen 1991; Friederici, 1995; Kerpez and Smith, 1987). During flood events, water flows over the expanded riverbanks and interacts with the dense saltcedar stands. The shrub's anchored structure renders it resistant to uprooting from strong currents and its structural presence increases water depth through flow resistance. Removal of saltcedar along an 18.5 km reach of the Gila River in Arizona resulted in a decrease of Manning's 'n' roughness coefficient, stage, and depth of peak discharges and mitigated flood damages that would have otherwise resulted if saltcedar was not removed (Burkham, 1976).

Saltcedar's primary root stem grows downward with minimal lateral extension until it reaches the water table (Horton, 1977). This characteristic is a major factor enabling it to outcompete native vegetation. Root characteristics also act as a controlling factor of saltcedar distribution, as their requirement to reach the water table leads to a majority of saltcedar concentrated on relatively flat floodplains with little elevation change (Everitt, 1980). Saltcedar's ability to draw moisture from both the saturated zone below the water table as well as unsaturated soils above deeper water tables provides an advantage over native vegetation with shallower root systems (Everitt, 1980). Most

native woody taxa are obligate phreatophytes and source their water from shallower water tables (Busch et al., 1992). The deeper root structure of saltcedar enables them to draw down the water table below the reach of many native species, which contributes to its competitive advantage and decline of native riparian vegetation (Brotherson et al., 1984).

Evapotranspiration (ET) rates of saltcedar far exceed that of native species and is among the most important factors driving management efforts in the southwest (van Hylckama, 1974; Brotherson et al., 1984). Their water usage is so extensive that they have been attributed to the complete drainage of hydric systems such as groundwater springs, pools, and perennial streams (Johnson, 1987). Numerous studies have attempted to quantify the amount of water used by *Tamarix* throughout their naturalized ranges and have resulted in varying estimates. Variation of water use has created divided opinions on management efforts. Shafroth et al. (2005) stated that “Despite decades of saltcedar invasion and control attempts, conflicting opinions remain about how, where, or if controlling saltcedar is likely to provide ecological or economic benefits that justify removal”. Site specific environmental and climatic factors may prove to be the source of varying estimates of saltcedar’s evapotranspiration. Riparian phreatophytes require access to water tables to consume the required amount of water for survival and growth, and shallower water tables give species such as saltcedar easier access to consume greater amounts of water (Robinson, 1965; van Hylckama, 1970, 1974; Davenport et al., 1982; Cooper et al., 2006). Solar radiation also controls the rates of ET, with notable decreases found during overcast days (Butler et al., 2007). Conversely, Davenport et al. (1982) found that saltcedar ET may not be accurately measured due to the plant’s increased

stomatal resistance during extremely hot temperatures in dry soil conditions and resulting water use quantities may be exaggerated. In this scenario, *Tamarix* will close their stomata during the hottest part of the afternoon to reduce water loss (Hagemeyer and Waisel, 1990). Other climatic conditions such as humidity, wind, and air temperature affect saltcedar ET (Gatewood et al., 1950; Robinson, 1965; Devitt et al., 1997). Gatewood et al. (1950) states saltcedar ET is at its lowest during humid conditions, something that is not common in many environments where saltcedar is located. Stand density has also been found to be a major contributing factor to saltcedar ET. Weeks et al. (1987) found significantly lower ET rates in scattered stands compared to stands moderately to densely packed. Regardless of stand density, saltcedar possesses a higher leaf area than native riparian species, allowing for higher rates of ET (Sala and Smith., 1996; Di Tomaso, 1998). Losses of water due to saltcedar are continuing to put stresses on their affected environments and is another reason for a decline in native riparian vegetation (Cleverley et al., 1997).

Displacement of native taxa through ecosystem alteration is an issue that management efforts are attempting to rectify. Riparian and wetland ecosystems are critically important to arid and semiarid environments of the western United States, as sources of sustenance to many native taxa (Sanders and Edge, 1998; Skagen et al., 1998). Riparian ecosystems support many endangered species, and these habitats are increasingly threatened by alteration and degradation caused by land development, pollution, water diversions, and exacerbated by invasive species (Allan and Flecker, 1993; Moyle, 1994; Dudley and Collins, 1995). Saltcedar water consumption displaces riparian-dependent native species. Avian species that live perennially or seasonally prefer

native cottonwood, willow and mesquite stands to saltcedar (Cohan et al., 1978). Ground nesting species have adapted to nesting within saltcedar stands, but a lack of preferred food sources has led to an increase of foraging in nearby agricultural fields (Brotherson and Field, 1987).

Changes to overall vegetation stand structure and composition have also negatively affected bird communities. Several native species of bird prefer stands of trees or shrubs between approximately 5 and 21 meters in height, which is taller than most saltcedar (Anderson et al., 1977). Reproductive fitness of birds who nest in saltcedar was also found to be significantly lower than species in native stands (DeLoach et al., 2000; Dudley et al., 2000). This decreased fitness is attributed to lower levels of food availability, as arthropod abundance has been reduced compared to similar ecosystems with more abundant native vegetation (Stevens, 1985, Delay et al., 1999; Knutson et al., 2003; Yard et al., 2004). Herpetofauna are also affected and occur in lower diversities and abundances in saltcedar dominated habitats (Jakle and Gatz 1985; Szaro and Belfit, 1986; Konkle, 1996). Many fish species that are regionally endemic to the west and southwest have been negatively affected by the alterations created by saltcedar invasion. Some species benefited from the removal of dense saltcedar and reversion to natural conditions (Kennedy, 2002). Effects on mammal populations have shown mixed results, as species-specific interactions with riparian habitats vary. Large mammals such as the Peninsular bighorn sheep (*Ovis canadensis cremnobates*) have seen their access to surface water reduced by saltcedar uptake (Rowlands, 1989; Lovich and DeGouvenain 1998). Some species of smaller mammals have seen their numbers remain unchanged, although saltcedar invasion was considered a major factor in the near elimination of

beaver and kangaroo rat in Big Bend National Park (Boer and Schmidly, 1977).

### **Management Techniques in Texas**

Saltcedar's effects on hydrology, geomorphology, and ecology created the need for management to eradicate the invader and restore native conditions. The assertion that saltcedar management will result in overall water gains appeals to communities and many keyholders and has led to management efforts throughout west Texas and other affected areas of the southwest (Mayes et al., 2019). Several studies, however, have only found modest water gains, and these findings have yet to be documented at a watershed scale (Wilcox 2002; Wilcox et al., 2006; Doody et al., 2011; Cleverly, 2013; McDonald et al., 2015). Although water gains have yet to be broadly substantiated, management of saltcedar can help to achieve flow restoration while protecting channel and riparian habitats from further degradation. Flow restoration and protection strategies prove to be the most feasible and impactful conservation objectives within west Texas (Valente et al., 2019).

Unlike other states where saltcedar infestation requires management, an overwhelming majority (95 percent) of affected habitat in Texas is privately owned. Watershed-scale efforts must engage and partner with private landowners in order to effectively manage saltcedar (Mayes et al., 2019). Outreach programs have aimed to educate landowners on the effects and threat of saltcedar. Beginning in 2015, the TPWD launched an initiative to combat *Tamarix* in the UBR, alongside USFWS and Texas A&M AgriLife Extension. Since their efforts began in 2016, these groups have treated more than 18,500 acres of saltcedar along the UBR on 140 ranches (TPWD, 2018). The



main treatment method in the UBR has involved targeted applications of the herbicide Imazapyr. A member of the imidazolinone family of herbicides, Imazapyr's effectiveness stems from its ability to inhibit the synthesis of enzymes vital for amino acid production (Mayes et al., 2019). Imazapyr has been deemed "practically nontoxic" to fish populations in aquatic formulas (Shaner and O'Connor, 1991). Application of Imazapyr in the UBR occurs via helicopter spraying of the saltcedar foliage. Helicopter-based application can be highly effective in the management of *Tamarix* (Duncan and McDaniel, 1998). Helicopters also provide a degree of maneuverability that cannot be achieved in fixed-wing aircraft, allowing applicators to avoid treating native species such as cottonwood (McDaniel and Taylor, 2003). Some detrimental effects of Imazapyr exist, with potential long-lasting consequences. Imazapyr applied via helicopter binds to the soil and is degraded mainly through microbial activity, thus creating an extended residence time that may inhibit the growth of native vegetation (Shaner and O'Connor, 1991; Mayes et al., 2019).

Biological agents have also been implemented in the management efforts of saltcedar within Texas, albeit not within the selected region of this study. Saltcedar beetles (*Diorhabda spp.*), a natural predator originating from the same native range of *Tamarix* have been used as a biological control agent. These beetles have been introduced throughout the United States, including Texas, to aid in the management of saltcedar (Bean et al., 2013). Per Bean et al. (2013), at least one species of this beetle is found in low numbers in the UBR watershed and are transient as they prefer to feed on new growths. Complete eradication of *Tamarix* is nearly impossible, treatment to date has required excessive expenditures and human intervention. Integrated herbicide and

biological management approaches could be best implemented in the small creeks and draws that are essentially inaccessible by air. After herbicide treatment, fresh new growth of saltcedar may seem more appetizing to the saltcedar beetles than older and denser stands (Mayes et al., 2019).

Due to saltcedar's extensive and dense coverage, complete eradication at a watershed scale is not an attainable goal. Instead, mimicking natural disturbances could prove to be the most effective management plans along with targeted herbicide applications. Manual removal of saltcedar and herbicidal treatment creates a fragmented environment, which in turn can create an opening for natural processes to begin the transition back to previous fluvial conditions (Mayes et al., 2019). Flood and high flow events are required to mobilize and transport sediment that has accumulated in the floodplains, removing the habitat needed for saltcedar expansion. Although the current channel-floodplain hinders the effectiveness of flood events, any high flow event in managed areas may become more effective for promoting natural instream habitat and improved river functions, and quality (Keller et al., 2014). Integrated management efforts of saltcedar could increase water gains from 5,600 to 10,800 L/ha treated within the upper reaches of the watershed at only a 10 percent reduction of saltcedar (Mayes et al., 2019). Similar results from Harwell et al. (2016) were calculated within the Double Mountain Fork upstream of Lake Alan Henry (Harwell et al., 2016).

### **Remote Sensing of *Tamarix* spp.**

Effective management efforts at a watershed scale could not be achieved without the proper understanding of saltcedar's areal extent and distribution. Remote sensing provides a means of detecting invasive species and quantifying rates of land cover change (Wang et al., 2013). Since the introduction of high-resolution satellites, data has been utilized in the identification of other invasive species in Texas such as giant reed (*Arundo donax*) and spiny aster (*Chloracantha*) (Everitt et al., 2005). Remote sensing of saltcedar has been explored in multiple studies, using hyperspectral imagery. Hamada et al. (2007) investigated saltcedar mapping using hyperspectral (0.5m) imagery in California, and Pu et al. (2008) conducted change detection calculations in saltcedar environments through NDVI differencing and traditional image classification (Hamada et al., 2007; Pu et al., 2008). Saltcedar's late fall to early winter variations in leaf color can serve as the basis of species identification (Everitt and DeLoach, 1990; Groeneveld and Watson, 2008; Diao and Wang, 2016). A technique that has been used frequently in mapping and quantifying cover change at a species level is the object-based image analysis (OBIA).

### **Utilization of OBIA for Mapping Riparian Vegetation**

Riparian study areas pose challenges for manual and pixel-based vegetation mapping due to narrow stream widths, seemingly erratic drainage patterns, and varied compositions (Yu et al., 2006). To overcome these obstacles, other approaches have been utilized. OBIA of remotely sensed imagery is based on grouping sets of similar pixels into image objects (Macfarlane et al., 2017). OBIA overcomes the shortcomings of other techniques for vegetation classification because it relies on spectral, spatial, textural, and

contextual information from the created image objects rather than spectral reflectance from individual pixels as the foundation of categorization (Blaschke et al., 2014). It is widely agreed that OBIA builds upon previous segmentation, edge-detection, feature extraction, and classification concepts that have been developed and refined over many decades of remote sensing studies (Haralick and Shapiro 1985; Hay et al., 2001; Burnett and Blaschke. 2003; Laliberte et al., 2004). OBIA has been used in various change detection studies (Lunneta et al., 2006; Ma et al., 2016). OBIA can be divided into two main steps: segmentation and classification. Image segmentation is often defined as a method for dividing an image into homogenous regions (Pal and Pal, 1993). Homogenous regions represent areas of the image of similar land cover (i.e., buildings, water, grass) that are known as image objects (Heumann, 2011; Costa et al., 2018). Segmentation is the most critical step in OBIA, and the accuracy of the following classification depends heavily on the quality of the segmentation algorithm (Mountrakis et al., 2011; Su and Zhang, 2017).

OBIA segmentation/classification of vegetated cover using high spectral resolution in RGB imagery can improve the mapping accuracy of small features, such as trees of different species or age (Platt and Rapoza, 2008). In imagery with a spatial resolution greater than 5 m per pixel, vegetation stands can be discerned on a coarse scale and below this threshold, vegetation can be discriminated on an individual basis (Blaschke et al., 2010). OBIA has been generally considered highly accurate (> 85 percent), and more efficient than pixel-based image analysis. In order to achieve a single-scale segmentation, the parameters and thresholds of that segmentation must be tuned to meet the requirements of the scale of study. It is often the case that determining the

correct scale in advance of the analysis is difficult as significant objects may appear at different spatial scales within the same image (Blaschke et al., 2010). In this study, the intended scale will be that at a tree stand scale, as that the structure of saltcedar communities within the UBR.

Application of select indices may help improve the accuracy of classification. Nguyen et al. (2018) applied two indices as masks to separate vegetation from other kinds of land covers. The Normalized Difference Water Index (NDWI) is used to separate water from other image objects, and the Normalized Difference Vegetation Index (NDVI) to separate bare soils from vegetation in arid environments. Select band ranges (642 – 683 nm and 750 – 870 nm) were determined to be important predictors for vegetation classification, as the range of spectra is related to the growth and vigor of plants. In addition to using hyperspectral imagery, random forest classification provided robust results even with a small sample size (94.8 percent overall accuracy) (Nguyen et al., 2018).

### III. METHODOLOGY

#### Study Area

The Brazos River flows for more than 2,000 km from the headwaters of the Blackwater and Yellow House Draws of southeastern New Mexico, eastward through central Texas, before turning south and emptying out into the Gulf of Mexico. The three selected areas are located on tributaries in the northwestern area of the Brazos River drainage basin. Two locations are on the North Fork Double Mountain Fork Brazos River (NFDMF) in northwestern Garza County, and one location is on the Double Mountain Fork Brazos River (DMF0) in southern Kent County (Figures 1-3). The three site locations are saltcedar management areas executed by TPWD and its partners since 2016.

Streamflow in these locations is highly variable and is dependent on rain events for much of the year (Echelle et al., 1972). Rainfall averages approximately 60 cm annually and falls in hard, localized showers. Sediment size found in the UBR ranges from clay to cobbles, creating braided channels that have since been affected by saltcedar growth. Alluvium within the floodplain is immature and is sourced from iron oxide rich red beds that are Permian to Triassic in age.

Vegetation is similar to other similar arid and semiarid ecosystems. Mesquite dominates much of the slopes and open areas in all three sites. Other shrubs such as hackberry occur at smaller frequencies. Saltcedar is located very close to the stream, though some were observed away from the stream if there was a wetted depression, or an arroyo that flows during precipitation. Saltcedar, both healthy and unhealthy, could be found in stands ranging from a single individual to very dense, extensive stands. Some

species were present at some sites while not at another. Cottonwoods were more prevalent at DMF 0 than the NFD MF sites. This presence could be explained by the slight increase in moisture from the NFD MF sites, southeast towards DMF 0. Grass types also differ between sites but were grouped into one class per image due to their similar spectral responses.

# North Fork Double Mountain Fork 1

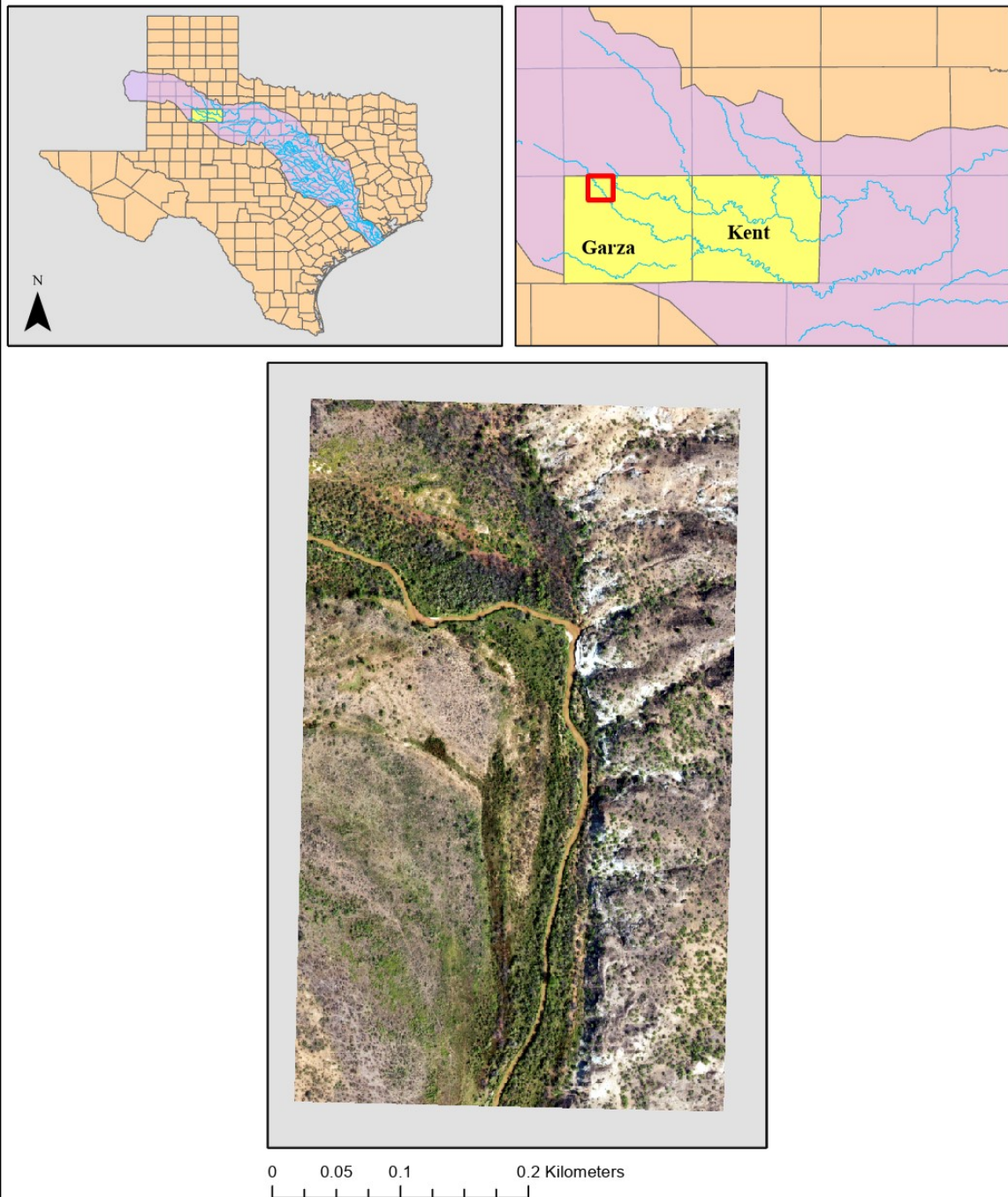


Figure 1. NAIP image of NDFMF 1



# North Fork Double Mountain Fork 2

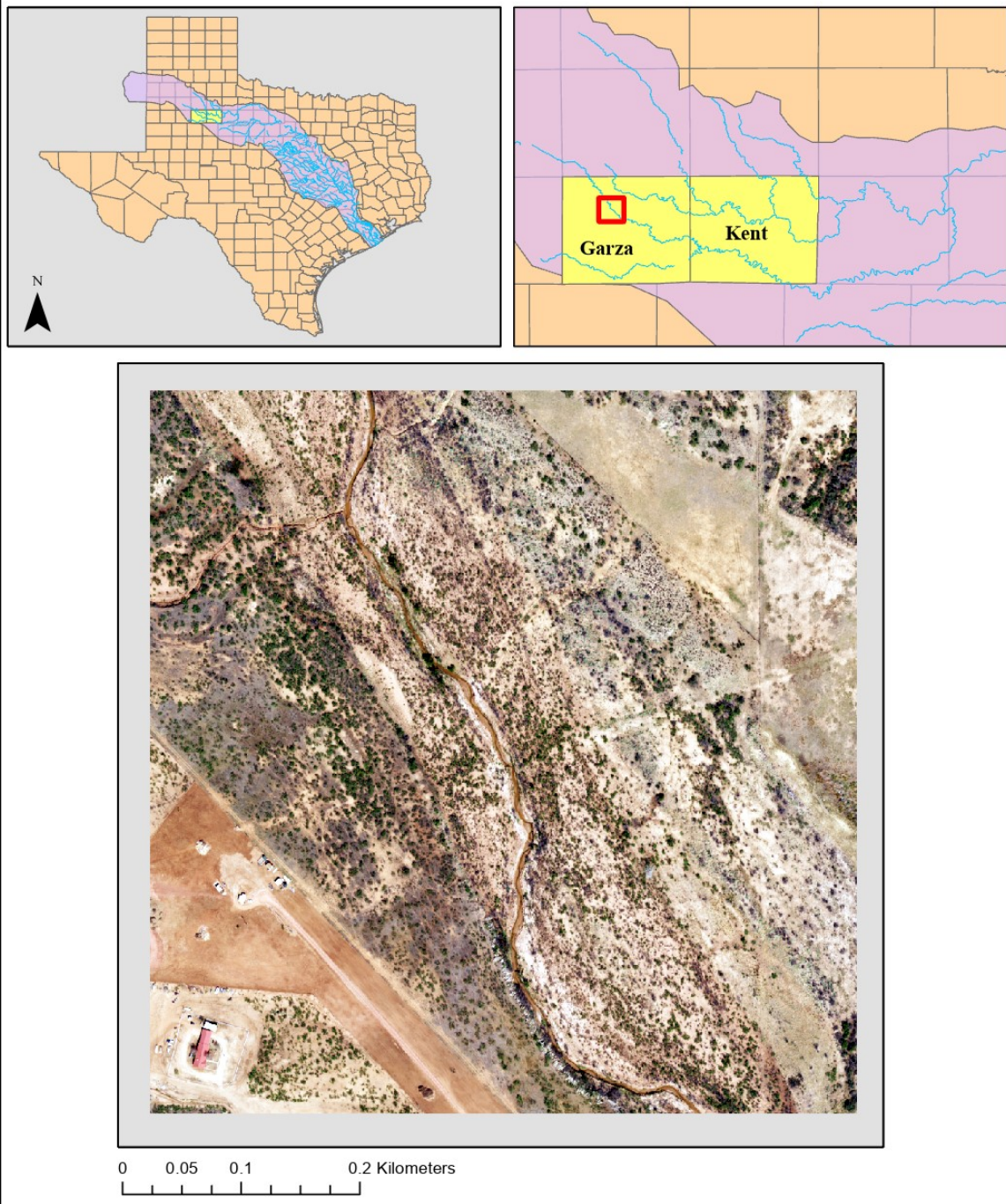
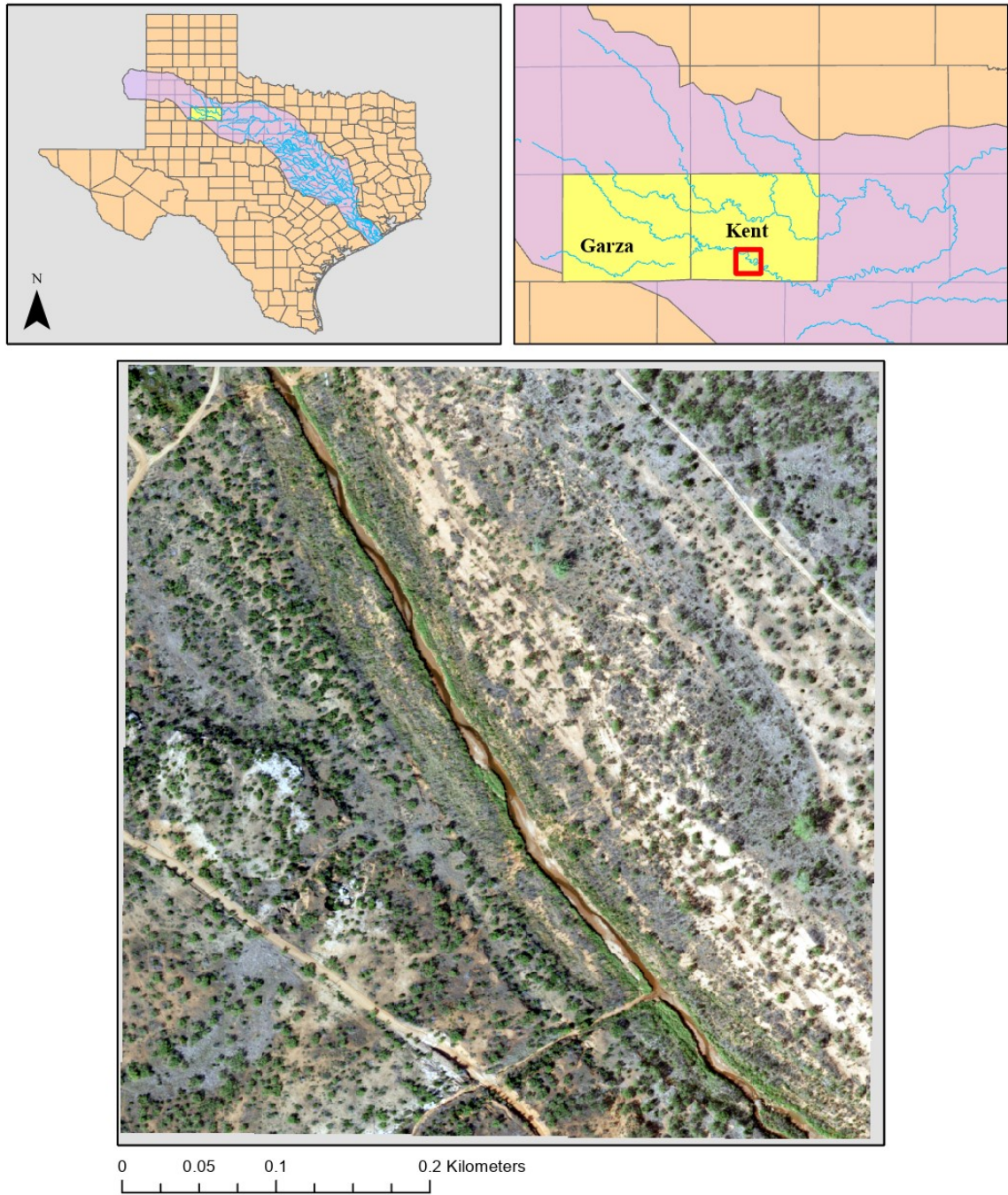


Figure 2. NAIP image of NFD MF 2

# Double Mountain Fork 0



## Data Collection

High spatial resolution imagery was collected to display areas of pre- and post-managed saltcedar treatments. The images of each section were collected as part of the National Agriculture Imagery Program (NAIP), which provides 1 x 1 m<sup>2</sup> spatial resolution for the United States during leaf on conditions. Spatial resolution improved to 60 cm per pixel beginning in 2018. Each individual tile is based on a 3.75 – minute longitude by 3.75 minute – latitude quarter quadrangle, including a 300-meter buffer on each side. Each image tile is orthorectified in the Universal Transverse Mercator (UTM) coordinate system, North American Datum 1983 (NAD 83), and cast into a single predetermined UTM zone. The images collected are color-infrared (CIR), containing red, green, blue, and near-infrared (NIR) bands. Instead of being captured via satellite, NAIP imagery is collected by the Leica ADS100 Aerial Scanner that is fixed to a commercially flown aircraft (U.S. Department of Agriculture, 2013). Images are taken under ideal weather conditions, containing no more than 10 percent cloud coverage per quadrangle. Imagery is orthorectified, and each tile image is contractually obligated to be horizontally accurate within 6 meters of ground control points. Imagery is available for download from the United State Geological Survey EarthExplorer image database for all selected locations. Collection of these images occurred for the years 2012 and 2020 (Table 1).

Table 1. Collection dates for NAIP imagery in 2012 and 2020.

Image	2012 Collection Date	2020 Collection Date
NFDMF 1	August 5 <sup>th</sup>	September 25 <sup>th</sup>
NFDMF 2	August 5 <sup>th</sup>	September 25 <sup>th</sup>
DMF 0	August 5 <sup>nd</sup>	September 27 <sup>th</sup>



Ground reference data was sourced using TPWD's Ecological Mapping Systems, which provides 10 m resolution land classifications for almost 400 various land cover designations. Derived from NAIP imagery, the vegetation cover class has an accuracy of 74 to 90 percent (TPWD, 2022). These classifications are visualized in TPWD's Texas Ecosystems Analytical Mapper (TEAM) that is supplemented by GroundTruther. This tool is a crowdsourced application that allows citizen scientists to provide feedback to TPWD on the accuracy of the vegetation classification, and aids in tracking changes in vegetative cover. GPS points were taken in the field at both NFD MF sites. These points were then used to help classify the images.

### **Data Preprocessing**

The initial step to preprocessing this data is to create an area of interest (AOI), focusing on the stream channel and adjoining areas and discarding the rest of the images. Exact AOIs in each location are selected for their habitat potential of saltcedar. Channel segments are relatively straight, and have wide, flat floodplains in which saltcedar hypothetically occurs in highest densities. Total extents of AOI from location to location varied, as their distinct morphologies influenced AOI creation. In order to explore the variance in accuracy between a larger area and a floodplain, an AOI of strictly the floodplain in NFD MF 1 was created. AOIs are then clipped from their respective images and exported as GeoTIFFs.

Originally, one goal of preprocessing was to convert the digital numbers of NAIP imagery into Top-of-Atmosphere (ToA) values. This removes some atmospheric alteration of the reflected wavelengths to produce more accurate and precise calculations

for desired indices. Digital numbers are a variable that is assigned to a pixel in the form of a binary integer to express values of reflectance. Digital numbers were not converted due to the extreme lack of relevant metadata needed to calculate radiance and reflectance. This conversion could have been accomplished with satellite imagery such as Landsat, but complications including temporal and instrumental restrictions disallowed this conversion to be used as a reference to the NAIP imagery.

Calculation of a NDVI layer for NAIP will be done to help identify vegetation covers and improve classification. Calculation of NDVI creates a dimensionless index that displays the difference between visible and NIR reflectance of vegetation cover and can be used to estimate the density of green vegetation (Weier and Herring, 2000). This calculation will be applied to all NAIP images through ArcGIS Pro. This raster function applies a band math equation included below.

$$\frac{(NIR - R)}{(NIR + R)}$$

Where NIR is the reflectance values associated with the near-infrared band, and R is the reflectance values associated with the red band. Bands necessary for NDVI calculation from NAIP imagery are bands 1 (red) and 4 (NIR). The new NDVI layers will then be stacked with their respective original CIR images to help with classification.

In order to minimize the effect of spectrally similar pixels of differing vegetation, a grey level co-occurrence measurement will be added to each image. Grey level co-occurrence matrices (GLCMs) are based on co-occurrence probabilities and provide a method to generate textures from spectrally similar features (Haralick, 1973). A GLCM will characterize the configuration of grey scales in an image and is used to analyze the variations in textures within an image (Sonka, 1999). Using GRASS GIS, a first-order

texture measurement will be conducted to help with object identification prior to segmentation. Entropy (ENT) is the measure chosen, as it will identify areas within the image where classification confusion may occur. Values of ENT were tested to produce the best texture variation between vegetation types with similar spectral reflectance values. The smaller window is chosen to depict variation between vegetation types. The resulting rasters were then stacked with the NDVI bands of their corresponding images, and then in turn stacked to the original 4 band CIR NAIP image. Each preprocessed image will contain the original four bands (red, green, blue, NIR), plus the GLCM of the calculated NDVI rasters.

### **Object-Based Image Classification**

OBIA identifies image objects based on similar spectral values based on color, texture, and tone through image segmentation. Segmentation will be accomplished by using ArcGIS Pro and requires user-selected parameters such as spectral detail, spatial detail, minimum segment size, and band indices. Segmentation parameters of NFD MF 1, NFD MF 1 floodplain, NFD MF 2, and DMF 0 for both image years are provided in the accompanying tables. All images were segmented using the red, NIR, and NDVI bands extracted from the composite images.

Table 2. Segmentation parameters for NFD MF 1 and NFD MF 1 floodplain

Image	Spectral Detail	Spatial Detail	Minimum Segmentation Size
NFD MF 1 2012	18	17	5
NFD MF 1 2020	18.5	18	5

Table 3. Segmentation parameters for NFDMF 2

Image	Spectral Detail	Spatial Detail	Minimum Segmentation Size
NFDMF 2 2012	19	18	5
NFDMF 2 2020	18.5	18	5

Table 4. Segmentation parameters for DMF 0

Image	Spectral Detail	Spatial Detail	Minimum Segmentation Size
DMF 0 2012	18.5	18	10
DMF 0 2020	18.5	18	10

Spectral input focuses on the weight of separation between objects based on color reflectance characteristics on a scale of 1.0 – 20.0 with step changes of 0.5 (ESRI, 2022). Lower values result in broader classes and more smoothing, while higher values are implemented in situations requiring the discrimination of objects with similar spectral characteristics. Spatial detail input focuses on the weight of separation between objects based on spatial influences. Lower values also result in broader and smoother classes, while higher values are used in situations where objects are spatially small and clustered (ESRI, 2022). As this study aims to map the spatial distribution of saltcedar that occurs in dense, thick stands, this parameter is also set to a high value. Values of spatial detail range from 1.0 – 20.0, with step changes of 1.0. Minimum segment size considers the size of each scene and prevents over segmentation of the image. Segments that are smaller than the chosen minimum are merged with the neighboring pixel they best fit with (ESRI, 2022). Stands of saltcedar can vary in width, thus the minimum segment size varies depending on the characteristics of each individual image scene to ensure creating image objects that capture both small, scarce stands as well as large, dense stands. The mean shift algorithm will then be applied to the images to create image objects.

After segmentation, training sets were created. Training sets are groupings of segments that correspond to a defined class within the classification schema the user is trying to create. In this study, the schema for this classification contains many of the same classes, but as each scene location is dynamic, some classes were added or omitted. Once the selected training segments were created, they were exported as shapefiles.

Table 5. Class categories and values for NFDMF 1 and NFDMF 1 floodplain

Class	Subclass	Class Code
Saltcedar	Healthy (11) Unhealthy (12)	10
Mesquite	N/A	20
Grasses	N/A	30
Non-Vegetated	N/A	40

Table 6. Class categories and values for NFDMF 2

Class	Subclass	Class Code
Saltcedar	Healthy (11) Unhealthy (12)	10
Mesquite	N/A	20
Willow	N/A	30
Hackberry	N/A	40
Grasses	N/A	50
Non-Vegetated	Barren (61) Human Structures (62)	60

Table 7. Class categories and values for DMF 0

Class	Subclass	Class Code
Saltcedar	Healthy (11) Unhealthy (12)	10
Mesquite	N/A	20
Cottonwood	N/A	30
Hackberry	N/A	40
Grasses	N/A	50
Barren		60



Afterwards, the images were classified utilizing the Image Classification tool in ArcGIS Pro, using the Random Trees Classifier. Random Trees is also known as Random Forests (RF), which is an image classification technique that creates a number of decision trees to determine the class an object most likely belongs to (Breiman, 2001). The classification trees are created by selecting a random subset of segments from the training segment groups that were produced by the user. These trees then branch out by the creation of rules. In ArcGIS Pro, five parameters are needed for input: Training Samples, Maximum Number of Trees, Maximum Tree Depth, Maximum Number of Samples per Class, and the Segmented Image. The shapefile of the created training segments serves as the training samples. The maximum number of trees represents the number of trees that will be used in the decision forest. When more trees are used, the greater potential there is for a more accurate classification (ESRI, 2022). Maximum tree depth is the definition of the number of rule branches within each tree. Maximum number of samples is implemented in the definition of each class. To use all training samples to train the classifier, zero was selected for the maximum number of samples. The segmented raster image became input for the classification of the NAIP image. Information for each classified image is provided in the accompanying table. The resulting classified raster provides two information fields: class name which describes the name of the class, and class value, an integer value that specifically states the total count of pixels within the classified image per each category.

Table 8. Random Forest image classification parameters

Image	Max # of Trees	Max Tree Depth	Max # of Samples per Class
NFDMF 1 2012	120	90	0
NFDMF 1 2020	120	90	0
NFDMF 2 2012	135	100	0
NFDMF 2 2020	135	100	0
DMF 0 2012	120	100	0
DMF 0 2020	120	100	0
NFDMF 1 2012 Floodplain	120	90	0
NFDMF 1 2020 Floodplain	120	90	0

### Accuracy Assessment

After each classified NAIP image was created, accuracy assessments were conducted. This assesses how well each classification compared to the reference data utilizing user image interpretation. An overall accuracy of 75 percent with a 5 percent error was targeted to ensure the classification was accurate enough to be implemented in further studies.

The most indicative accuracy coefficient is Kappa, which determines the level of agreement. Kappa coefficients range from 0.00 – 1.00 which are categorized into 5 levels of agreement: slight (0.01 – 0.20), fair (0.21 – 0.40), moderate (0.41 – 0.60), substantial (0.61 – 0.80), and almost perfect (0.81 – 1.00) (Landis and Koch, 1977). A Kappa of at least 0.61 was targeted to demonstrate a substantial agreement of the classification. Jensen's (2004) multinomial distribution equation (MDE) was applied to determine the number of samples needed to perform an accuracy assessment.

$$N = \frac{B\Pi_i(1 - \Pi_i)}{b_i^2}$$

Where:

$$B = \left(\alpha/k\right) * 100$$

Where N represents the number of samples, B represents the Chi-square critical value for  $\alpha$  (alpha) divided by k, then multiplied by 100. Alpha represents one minus the desired confidence for the map. This study aims for a 75 percent Kappa coefficient, therefore alpha is  $1 - 0.75$ . Variable k is the total number of classes in this study, which varies between image scenes. This number is then multiplied by 100, and the product is used in a chi-squared right-tail distribution table with one degree of freedom.  $\Pi_i$  represents the class whose proportion of the map is closest to the majority of the image, and  $b_i$  represents the desired precision. Within this study, the precision was chosen at five percent.

Using the Zonal Histogram tool, raster values will be obtained from the classified data set from each image. Every class is then divided by the total pixel count to calculate the proportions of each class used in the MDE. Following this step, the MDE will be calculated. Because images and resolutions vary between image dates and location, the proportion of classes will vary as well. Due to this variation, the number of samples needed will vary between image products. Stratified random sampling will be used proportionally among all classification designations to derive the number of samples from each classified image needed to perform the accuracy assessment. Sample requirements will be provided in the accompanying table.

Table 9. Minimum number of sample points required for accuracy assessment using MDE

Image	Number of samples required
NFDMF 1 2012	374
NFDMF 1 2020	335
NFDMF 2 2012	447
NFDMF 2 2020	451
DMF 0 2012	416
DMF 0 2020	416
NFDMF 1 2012 floodplain	338
NFDMF 1 2020 floodplain	326

Once the number of sample points required for the accuracy assessment were calculated, the points are then created using the Create Accuracy Assessment tool in ArcGIS Pro. Visual interpretations of each sample points are made, then assigned a reference value. Once all points are assigned a reference value, the Compute Confusion Matrix tool will be used to calculate accuracy statistics of each classification. Statistics produced by the creation of a confusion matrix are producer accuracy, user accuracy, overall accuracy, and the overall Kappa coefficient. Producer accuracy refers to the effectiveness of the user produced classification schema. Omission errors from producer's accuracy defines the percentage of pixels omitted from the correct classification. User accuracy measures how well the data aids the user, and commission errors define the pixels that are included in a class they do not belong to. Overall accuracy describes the percentage of correctly classified objects within a segmented image. Kappa measures the degree of agreement within a classified image compared to the reference data and determines if the agreement occurs by chance. As the coefficient is described on a scale of 0 – 1, the closer the Kappa coefficient is to 1, the stronger the degree of agreement between the classified image and the reference data. As the classification was tuned to produce a satisfactory statistical outcome, change detection

calculations of saltcedar between image dates were conducted.

### **Stratified Image Approach**

Image stratification was incorporated to test its effect on improving the accuracy of both image classification using OBIA techniques and change detection of healthy to unhealthy saltcedar. Treating an image as a whole may not be helpful in identifying saltcedar as it occurs in only the floodplain, and not in other regions of the image that are not suitable for saltcedar. Stratifying an image to the floodplain may help to focus on the patterns of distribution in riparian vegetation, a phenomenon that is scale-dependent. Most segmentation procedures in studies using OBIA occur for the entire image and may not allow for the proper segmentation of heterogeneous regions of an image. As it is increasingly difficult to recognize spatial patterns in high-resolution imagery, the implementation of stratification was useful in extracting objects seen only in the floodplain (Zhou et al., 2018). Another approach could be to take the already classified image and clipping the extent to the stratified floodplain of the image to better constrain the area of change detection.

### **Change Detection**

A change detection was conducted between the classified images from August 2012 and September 2020. As the spatial resolution of the color infrared images was reduced from 1 m in 2012 to 60 cm in 2020, the images were resampled to a similar resolution for proper comparison. Image resampling adhered to the 2012 image resolution since it was coarser than the 2020 resolution. September 2020 image rasters were

resampled using the Resample tool, which utilizes the nearest neighbor technique for resampling in ArcGIS Pro. Under nearest neighbor, the value of the cells are not changed and alterations to the pixel values are minimized.

Change detection between the classified images was accomplished with the use of ArcGIS Pro's Change Detection Wizard tool, with categorical change. This tool takes two rasters representing the specified time difference (in this study, August 2012 to September 2020). The next step is the configure step, which identifies the classes used for change detection, which was the coverage of saltcedar. Symbolization of change was selected under the configure window. Within this window, the Transition Class Color Method provides specific details as to how the changed pixels will be visualized. Due to this change detection being between years, the 'to color' option was selected for change symbolization. No inputs were applied in the post-processing window to leave pixels unchanged from potential smoothing. The resulting images were then exported as rasters and feature classes.

Although this study aimed to detect the change in saltcedar from healthy to unhealthy, it could also be useful to understand areas where healthy saltcedar has not changed between 2012 and 2020. Detecting unchanged pixels can help to visualize areas of tenacious growth. Information such as this can also inform managers of areas where more focused efforts would be beneficial. This was achieved by using the Change Detection Wizard and selecting the categorical change of unchanged pixels of unhealthy saltcedar between the 2012 and 2020 classified images.

## IV. RESULTS

### Image Classification

Eight OBIA classified images were produced (Figures 4 – 11). The classes and pixel counts varied between each image site (Tables 10 – 17). From the pixel counts, the resulting coverage percentages were input into the MDE for accuracy assessment creation.

Table 10. Class counts and percentages for NFD MF 1 2012

Class	Total # of pixels	Percentage of coverage
Healthy Saltcedar	14,483	7.86%
Unhealthy Saltcedar	3,904	2.12%
Mesquite	76,689	41.62%
Grasses, Sedges and Baccharis	14,602	7.92%
Barren	74,601	40.48%

Table 11. Class counts and percentages for NFD MF 1 2020

Class	Total # of pixels	Percentage of coverage
Healthy Saltcedar	25,826	5.05%
Unhealthy Saltcedar	122,825	23.99%
Mesquite	158,572	30.98%
Grasses, Sedges and Baccharis	40,580	7.94%
Barren	164,089	32.06%

Table 12. Class counts and percentages for NFD MF 2 2012

Class	Total # of pixels	Percentage of coverage
Healthy Saltcedar	10,915	3.01%
Unhealthy Saltcedar	24,826	6.85%
Mesquite	43,748	12.07%
Willow	278	0.08%
Hackberry	44,387	12.25%
Grasses, Sedges, and Baccharis	15,273	4.21%
Barren	221,500	61.13%
Human Structures	1,441	0.40%

Table 13. Class counts and percentages for NFD MF 2 2020

Class	Pixel count	Percentage of coverage
Healthy Saltcedar	13,118	1.30%
Unhealthy Saltcedar	184,038	18.27%
Mesquite	77,682	7.72%
Willow	2,949	0.29%
Hackberry	106,110	10.54%
Grasses, Sedges, and Baccharis	10,651	1.06%
Barren	609,324	60.52%
Human Structures	3,008	0.30%

Table 14. Class counts and percentages for DMF 0 2012

Class	Total # of pixels	Percentage of coverage
Healthy Saltcedar	14,550	5.98%
Unhealthy Saltcedar	17,930	7.37%
Mesquite	18,789	7.72%
Cottonwood	1,744	0.72%
Hackberry	25,312	10.41%
Grasses, Sedges, and Baccharis	29,427	12.10%
Barren	135,475	55.70%

Table 15. Class counts and percentages for DMF 0 2020

Class	Total # of pixels	Percentage of coverage
Healthy Saltcedar	13,115	1.99%
Unhealthy Saltcedar	291,859	44.39%
Mesquite	62,295	9.47%
Cottonwood	12,072	1.84%
Hackberry	21,781	3.31%
Grasses, Sedges, and Baccharis	42,449	6.46%
Barren / Alluvium	231,967	35.28%

Table 16. Class counts and percentages for NFD MF 1 2012 floodplain

Class	Total # of pixels	Percentage of coverage
Healthy Saltcedar	16,606	20.98%
Unhealthy Saltcedar	13,378	16.90%
Mesquite	9,661	12.20%
Grasses, Sedges, and Baccharis	13,684	17.29%
Non-Vegetated	25,834	32.63%



Table 17. Class counts and percentages for NFDMF 1 2020 floodplain

Class	Total # of pixels	Percentage of coverage
Healthy Saltcedar	43,245	19.66%
Unhealthy Saltcedar	42,275	19.22%
Mesquite	26,258	11.94%
Grasses, Sedges, and Baccharis	41,187	18.73%
Non-Vegetated	66,970	30.45%

## North Fork Double Mountain Fork 1 2012 OBIA Classification

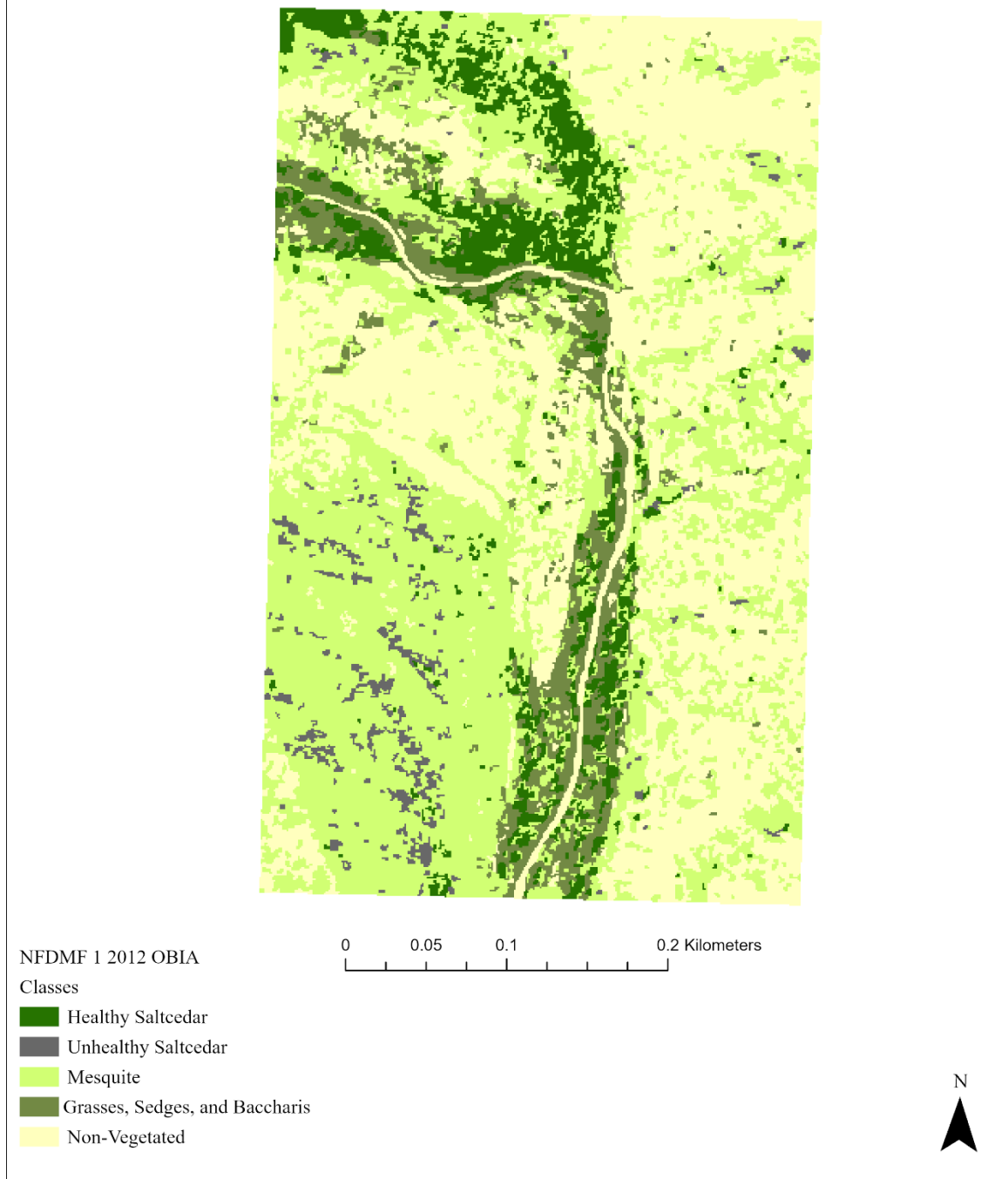


Figure 4. Classified map for NFD MF 1 2012

### North Fork Double Mountain Fork 1 2020 OBIA Classification

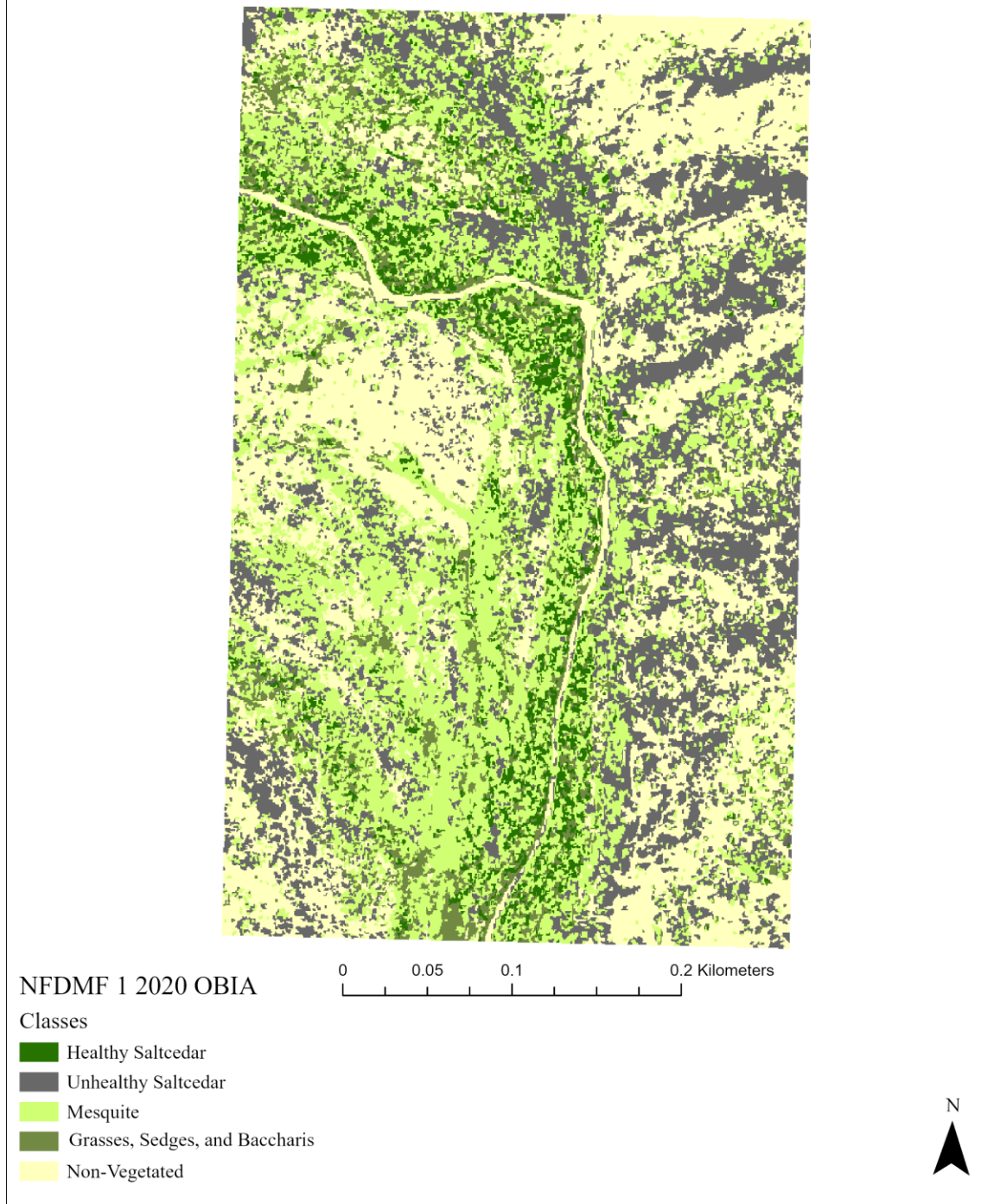
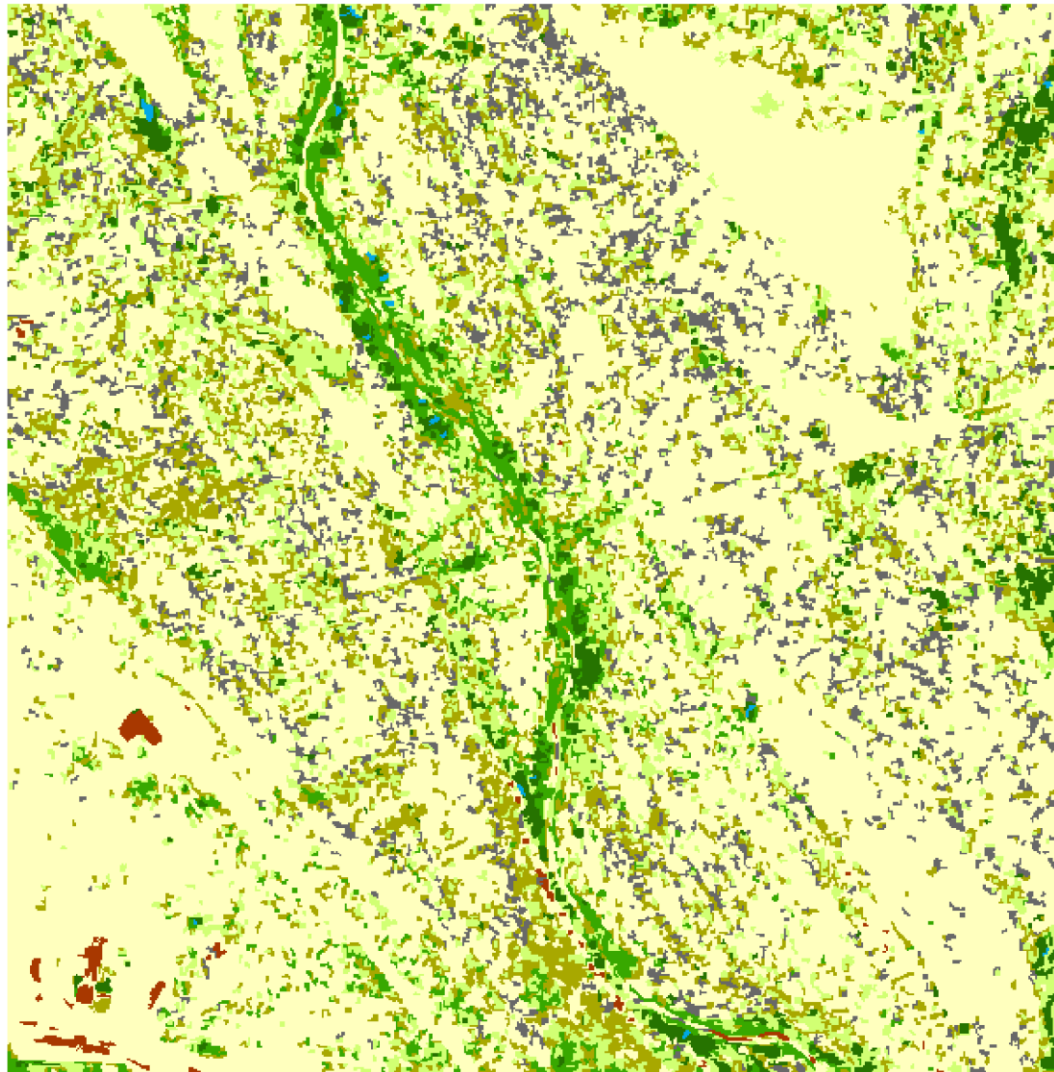


Figure 5. Classified map of NFD MF 1 2020

### North Fork Double Mountain Fork 2 2012 OBIA Classification



NFDMF 2 2012 OBIA

Classes

- Healthy
- Unhealthy
- Mesquite
- Willow
- Hackberry
- Grasses, Sedges, and Baccharis
- Barren
- Human Structures

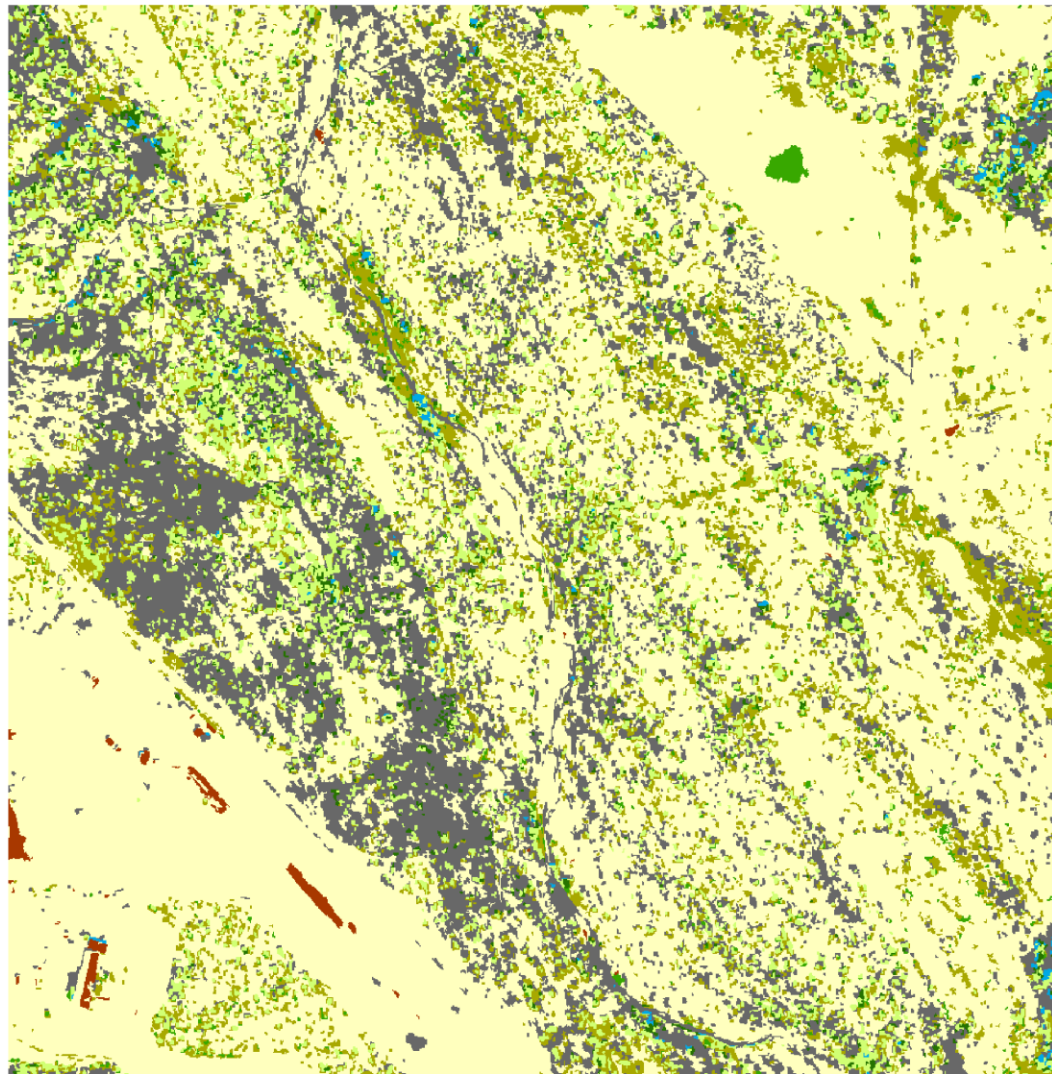
0 0.05 0.1 0.2 Kilometers



Figure 6. Classified map of NFDMF 2 2012



### North Fork Double Mountain Fork 2 2020 OBIA Classification



NFDMF 2 2020 OBIA

Classes

- Healthy
- Unhealthy
- Mesquite
- Willow
- Hackberry
- Grasses, Sedges, and Baccharis
- Barren
- Human Structures

0 0.05 0.1 0.2 Kilometers



Figure 7. Classified map of NFDMF 2 2020

### Double Mountain Fork 0 2012 OBIA Classification

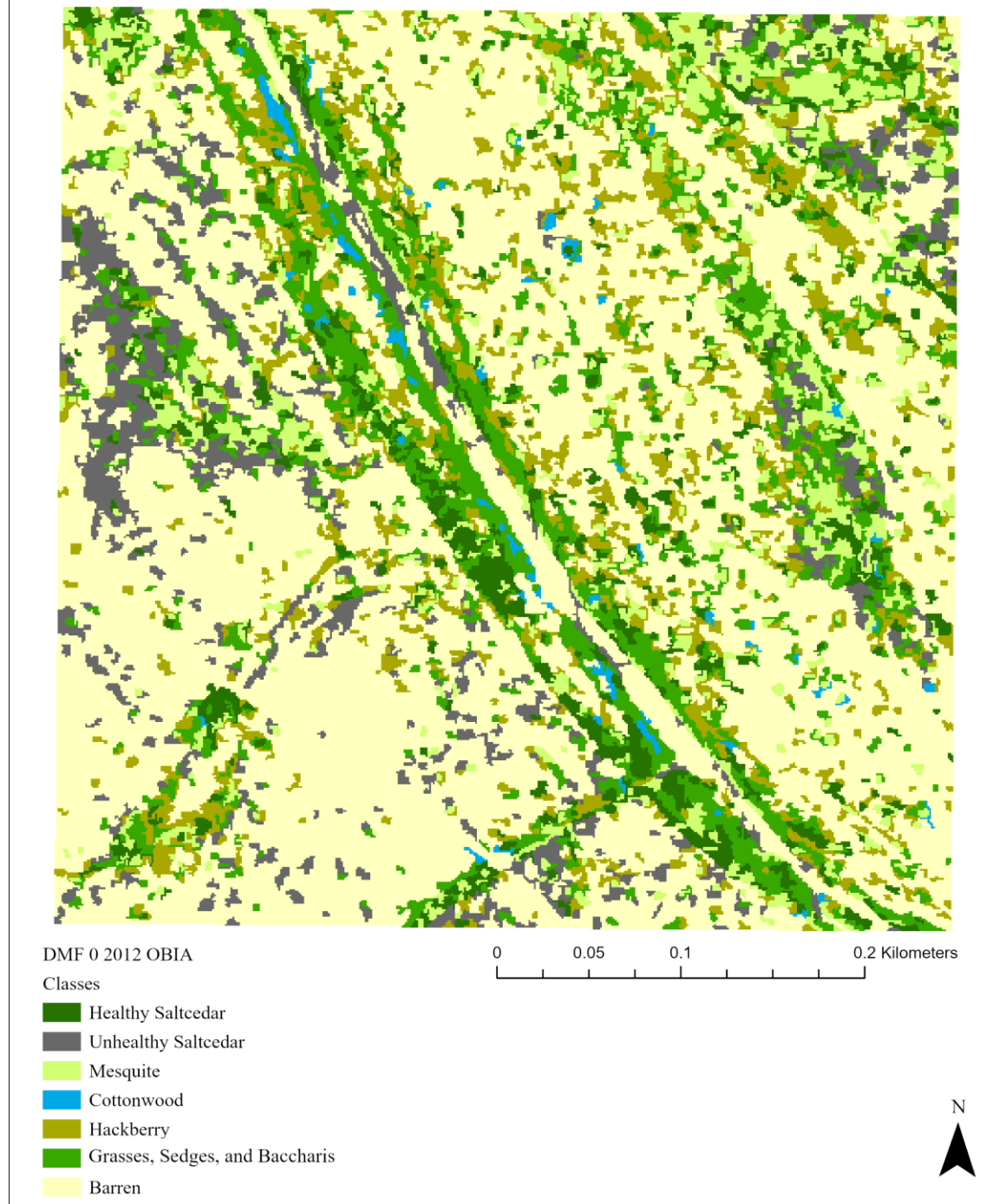
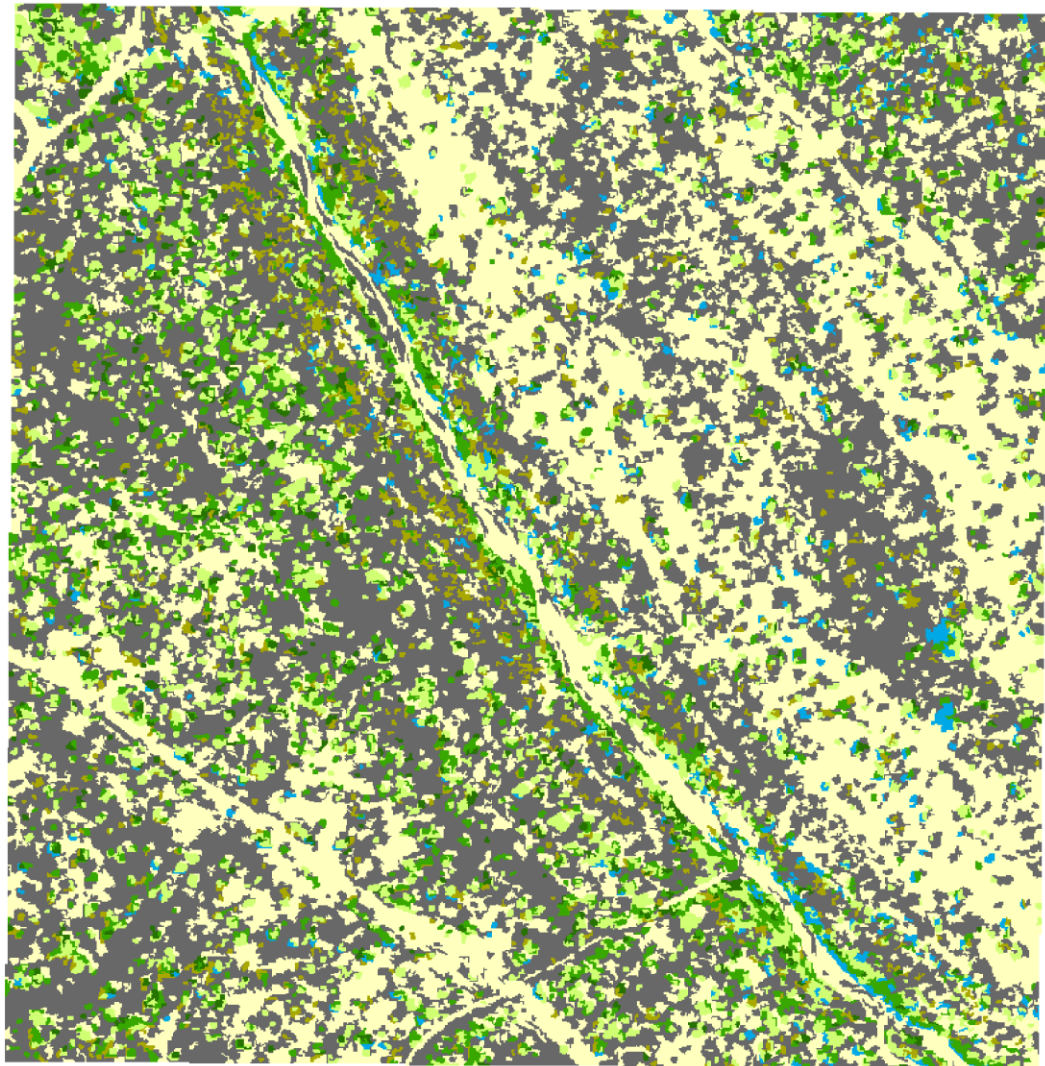


Figure 8. Classified map of DMF 0 2012

### Double Mountain Fork 0 2020 OBIA Classification



DMF 0 2020 OBIA

Classes

- Healthy Saltcedar
- Unhealthy Saltcedar
- Mesquite
- Cottonwood
- Hackberry
- Grasses, Sedges, and Baccharis
- Barren

0 0.05 0.1 0.2 Kilometers



Figure 9. Classified map of DMF 0 2020

# North Fork Double Mountain Fork 1 2012 Floodplain OBIA Classification

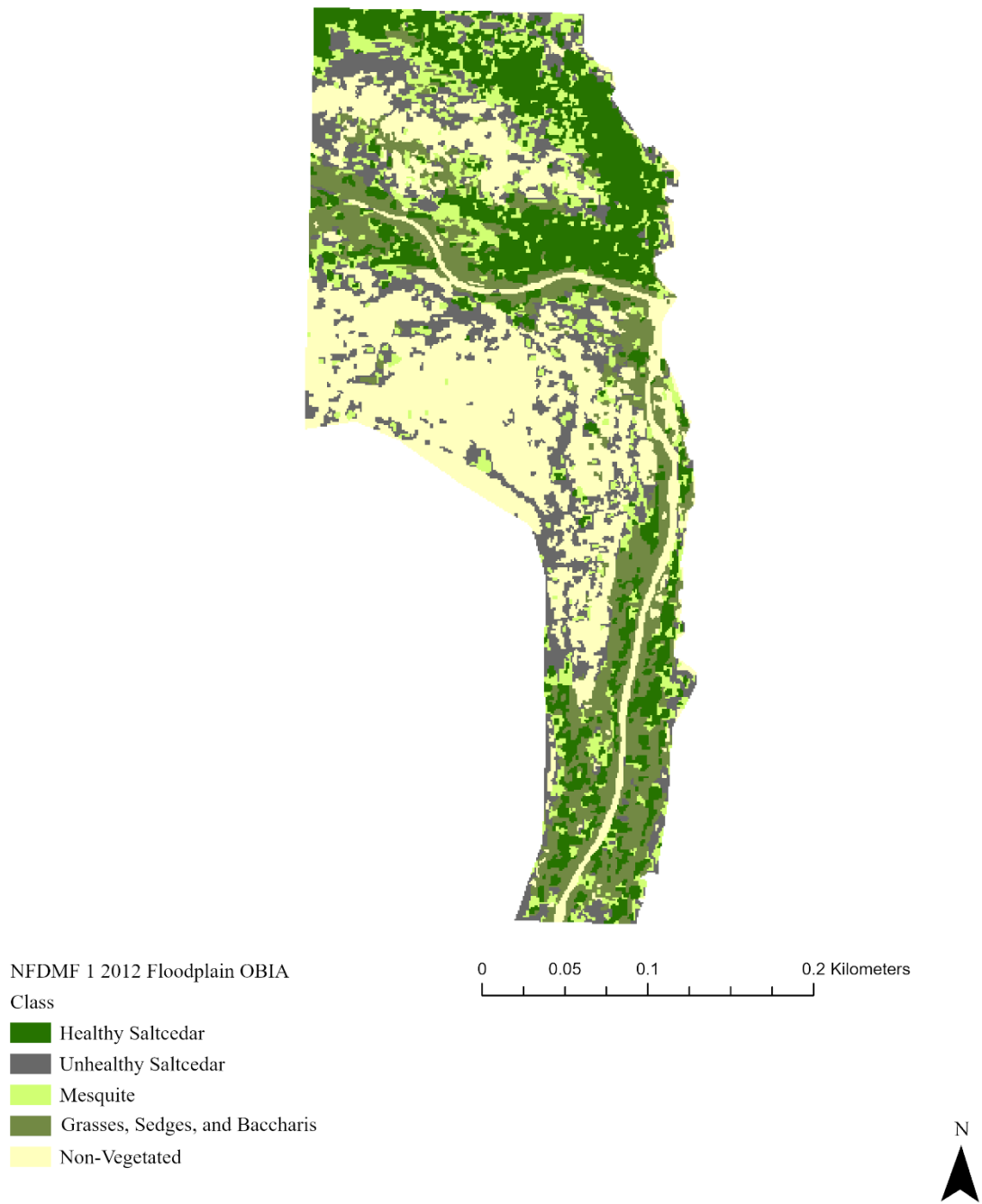


Figure 10. Classified map of NFD MF 1 2012 floodplain



# North Fork Double Mountain Fork 1 2020 Floodplain OBIA Classification

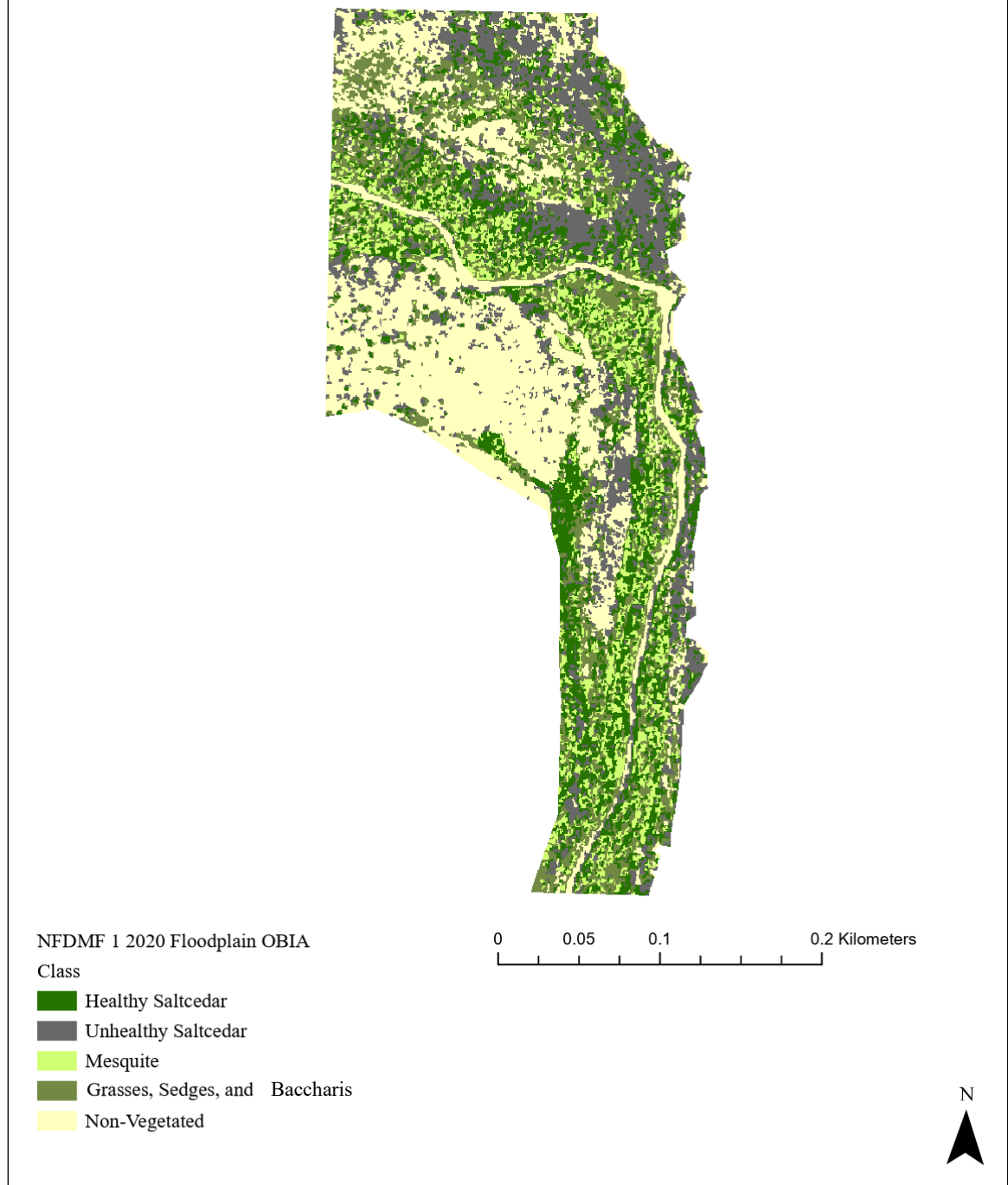


Figure 11. Classified map of NFD MF 1 2020 floodplain

## **Accuracy Assessments**

Summary accuracy statistics provide numerical representation of the classification. Confusion matrices assess which class sample points were assigned, and how they were classified using the created accuracy assessment points (Tables 18-25). Values within the tables include user accuracy, producer accuracy, and Kappa coefficients. Values also include the accuracies of classification by class. Using Table 18 as an example, the first row will demonstrate how well healthy saltcedar was classified for NFD MF 1 2012. Of the 29 sampled points of healthy saltcedar, 24 of them were correctly classified, resulting in a user accuracy of 82.75% (Table 16). As the change in saltcedar coverage is the focus of this study, it is important to understand how well the images were classified regarding these two classes. Six of eight accuracy assessments returned values above the desired overall accuracies and Kappa coefficients.

Table 18. Accuracy assessment for classified NFD MF 1 2012

Class	Healthy Saltcedar	Unhealthy Saltcedar	Mesquite	Grasses	Barren	Total	User Accuracy	Kappa
Healthy Saltcedar	24	0	4	1	0	29	82.75%	
Unhealthy Saltcedar	0	1	2	3	4	10	10.00%	
Mesquite	2	0	117	16	21	156	75.00%	
Grasses	1	0	5	24	0	30	80.00%	
Non-Vegetated	0	0	18	12	121	151	80.13%	
Total	27	1	146	56	146	376		
Producer Accuracy	88.88%	100.00%	80.13%	42.85%	82.87%		76.30%	
Kappa								0.64

Table 19. Accuracy assessment for classified NFDMF 1 2020

Class	Healthy Saltcedar	Unhealthy Saltcedar	Mesquite	Grasses	Barren	Total	User Accuracy	Kappa
Healthy Saltcedar	13	0	1	3	0	17	76.48%	
Unhealthy Saltcedar	2	40	10	6	22	80	50.00%	
Mesquite	2	5	72	18	7	104	69.23%	
Grasses	0	0	6	21	0	27	77.77%	
Non-Vegetated	0	0	11	12	84	107	78.50%	
Total	17	45	100	60	113	335		
Producer Accuracy	76.47%	88.88%	72.00%	35.00%	74.33%		68.65%	
Kappa								0.58

Table 20. Accuracy assessment for classified NFDMF 2 2012

Class	Healthy Saltcedar	Unhealthy Saltcedar	Mesquite	Willow	Hackberry	Grasses	Barren	Human Structures	Total	User Accuracy	Kappa
Healthy Saltcedar	10	0	2	0	0	0	1	0	13	76.90%	
Unhealthy Saltcedar	0	14	5	1	1	3	7	0	31	45.20%	
Mesquite	0	0	45	0	0	7	2	0	54	83.33%	
Willow	3	0	0	6	0	1	0	0	10	60.00%	
Hackberry	0	2	7	0	38	5	3	0	55	69.09%	
Grasses	0	0	2	0	2	15	0	0	19	78.94%	
Barren	0	0	20	0	2	13	238	0	273	87.17%	
Human Structures	0	0	0	0	0	0	7	3	10	30.00%	
Total	13	16	81	7	43	44	258	3	465		
Producer Accuracy	76.92%	87.50%	55.55%	85.71%	88.37%	34.09%	92.22%	100.00%		79.35%	
Kappa											0.68

Table 21. Accuracy assessment for classified NFDMF 2 2020

Class	Healthy Saltcedar	Unhealthy Saltcedar	Mesquite	Willow	Hackberry	Grasses	Barren	Human Structures	Total	User Accuracy	Kappa
Healthy Saltcedar	6	0	4	0	0	0	0	0	10	60.00%	
Unhealthy Saltcedar	0	47	6	0	1	1	27	0	82	57.31%	
Mesquite	0	1	28	0	4	1	1	0	35	80.00%	
Willow	1	0	2	7	0	1	0	0	10	70.00%	
Hackberry	0	2	4	0	29	4	8	1	48	60.41%	
Grasses	0	0	1	0	2	6	1	0	10	60.00%	
Barren	0	6	8	0	15	2	242	0	273	88.64%	
Human Structures	0	0	0	0	0	0	6	4	10	40.00%	
Total	7	56	53	7	51	14	285	5	478		
Producer Accuracy	85.71%	83.92%	52.83%	100.00%	56.86%	42.85%	84.91%	80.00%		77.19%	
Kappa											0.63

Table 22. Accuracy assessment for classified DMF 0 2012

Class	Healthy Saltcedar	Unhealthy Saltcedar	Mesquite	Cottonwood	Hackberry	Grasses	Barren	Total	User Accuracy	Kappa
Healthy Saltcedar	20	0	4	0	0	1	0	25	80.00%	
Unhealthy Saltcedar	0	19	2	0	0	3	6	30	63.33%	
Mesquite	3	1	24	0	1	3	0	32	75.00%	
Cottonwood	0	0	1	4	0	4	1	10	40.00%	
Hackberry	0	1	3	0	26	10	3	43	60.45%	
Grasses	1	2	10	0	3	33	1	50	66.00%	
Barren	0	4	4	0	14	8	201	231	87.01%	
Total	24	27	48	4	44	62	212	421		
Producer Accuracy	83.33%	70.37%	50.00%	100.00%	59.09%	53.22%	94.81%		77.67%	
Kappa										0.67

Table 23. Accuracy assessment for classified DMF 0 2020

Class	Healthy Saltcedar	Unhealthy Saltcedar	Mesquite	Cottonwood	Hackberry	Grasses	Barren	Total	User Accuracy	Kappa
Healthy Saltcedar	7	0	2	0	0	1	0	10	70.00%	
Unhealthy Saltcedar	0	105	20	0	4	10	41	180	58.33%	
Mesquite	0	1	32	0	3	2	0	38	84.21%	
Cottonwood	0	0	1	5	2	2	0	10	50.00%	
Hackberry	0	1	3	0	7	1	1	13	53.84%	
Grasses	0	1	8	1	1	15	0	26	57.69%	
Barren	0	8	6	0	2	6	121	143	84.61%	
Total	7	116	72	6	19	37	163	420		
Producer Accuracy	100.00%	90.51%	44.44%	83.33%	36.84%	40.54%	74.23%		69.52%	
Kappa										0.58



Table 24. Accuracy assessment for classified NFD MF 1 2012 floodplain

Class	Healthy Saltcedar	Unhealthy Saltcedar	Mesquite	Grasses	Non-Vegetated	Total	User Accuracy	Kappa
Healthy Saltcedar	56	0	10	5	0	71	78.87%	
Unhealthy Saltcedar	0	11	1	12	33	57	19.30%	
Mesquite	8	0	28	5	0	41	68.30%	
Grasses	5	0	4	47	2	58	81.03%	
Non-Vegetated	0	0	1	3	106	110	96.36%	
Total	69	11	44	72	141	337		
Producer Accuracy	81.20%	100.00%	63.64%	65.28%	75.18%		73.59%	
Kappa								0.65

Table 25. Accuracy assessment for classified NFD MF 1 2020 floodplain

Class	Healthy Saltcedar	Unhealthy Saltcedar	Mesquite	Grasses	Non- Vegetated	Total	User Accuracy	Kappa
Healthy Saltcedar	44	5	8	6	1	64	68.75%	
Unhealthy Saltcedar	1	44	6	2	10	63	69.84%	
Mesquite	3	1	29	5	1	39	74.36%	
Grasses	0	0	9	51	1	61	83.61%	
Non- Vegetated	0	2	2	9	86	99	86.87%	
Total	48	52	54	73	99	326		
Producer Accuracy	91.66%	84.62%	53.70%	69.86%	86.87%		77.91%	
Kappa								0.71

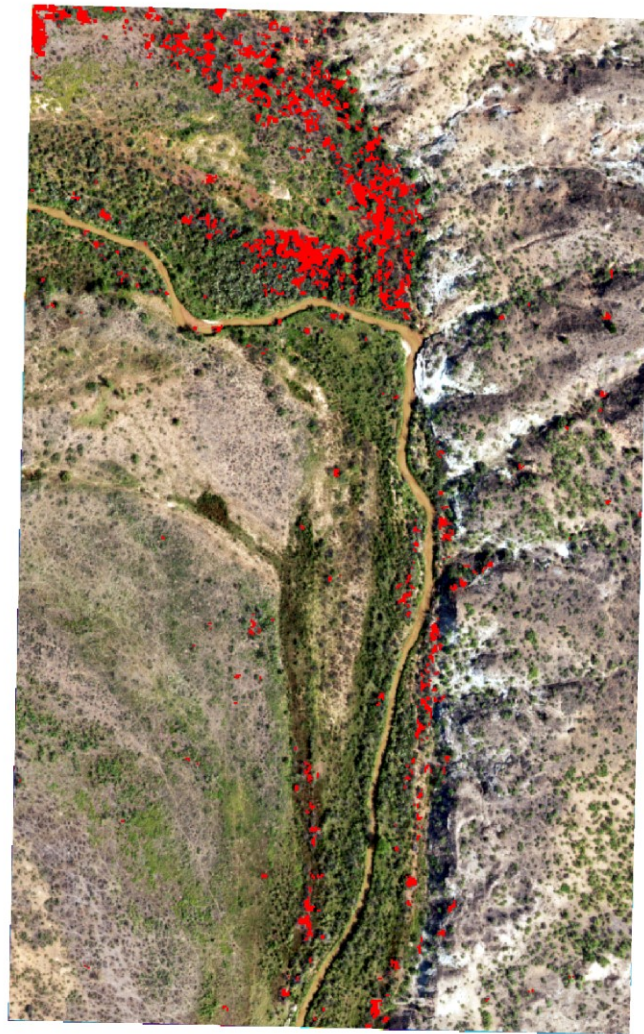
## Change Detection

As this study focuses on the change of saltcedar coverage, the change detection of healthy saltcedar to unhealthy is highlighted. The pixel-based change detection confirms a slight decline in saltcedar (Table 26) which can be visualized in the maps for the study areas, as well as areas where healthy saltcedar has persisted between 2012 and 2020 (Figures 12 – 19).

Table 26. Changed pixels and percent change of saltcedar

Image	# of changed pixels	Percent change
NFDMF 1	4,213	-2.34%
NFDMF 2	3,861	-1.08%
DMF 0	7,225	-3.06%
NFDMF 1 floodplain	6,152	-7.80%

## North Fork Double Mountain Fork 1 Change Detection



0 0.05 0.1 0.2 Kilometers

 Healthy Saltcedar to Unhealthy Saltcedar



Figure 12. Change detection of saltcedar for NFD MF 1

The bright red areas on each map are areas that were classified as healthy saltcedar in 2012 but were then reclassified to unhealthy saltcedar in 2020.

### North Fork Double Mountain Fork 1 Change Detection



0 0.05 0.1 0.2 Kilometers


 Unchanged Saltcedar



Figure 13. Change detection of unchanged saltcedar for NFD MF 1

The bright green areas on each map are areas that were classified as healthy saltcedar in 2012 and were classified as healthy saltcedar in 2020.



## North Fork Double Mountain Fork 2 Change Detection



Figure 14. Change detection of saltcedar for NFD MF 2



### North Fork Double Mountain Fork 2 Change Detection



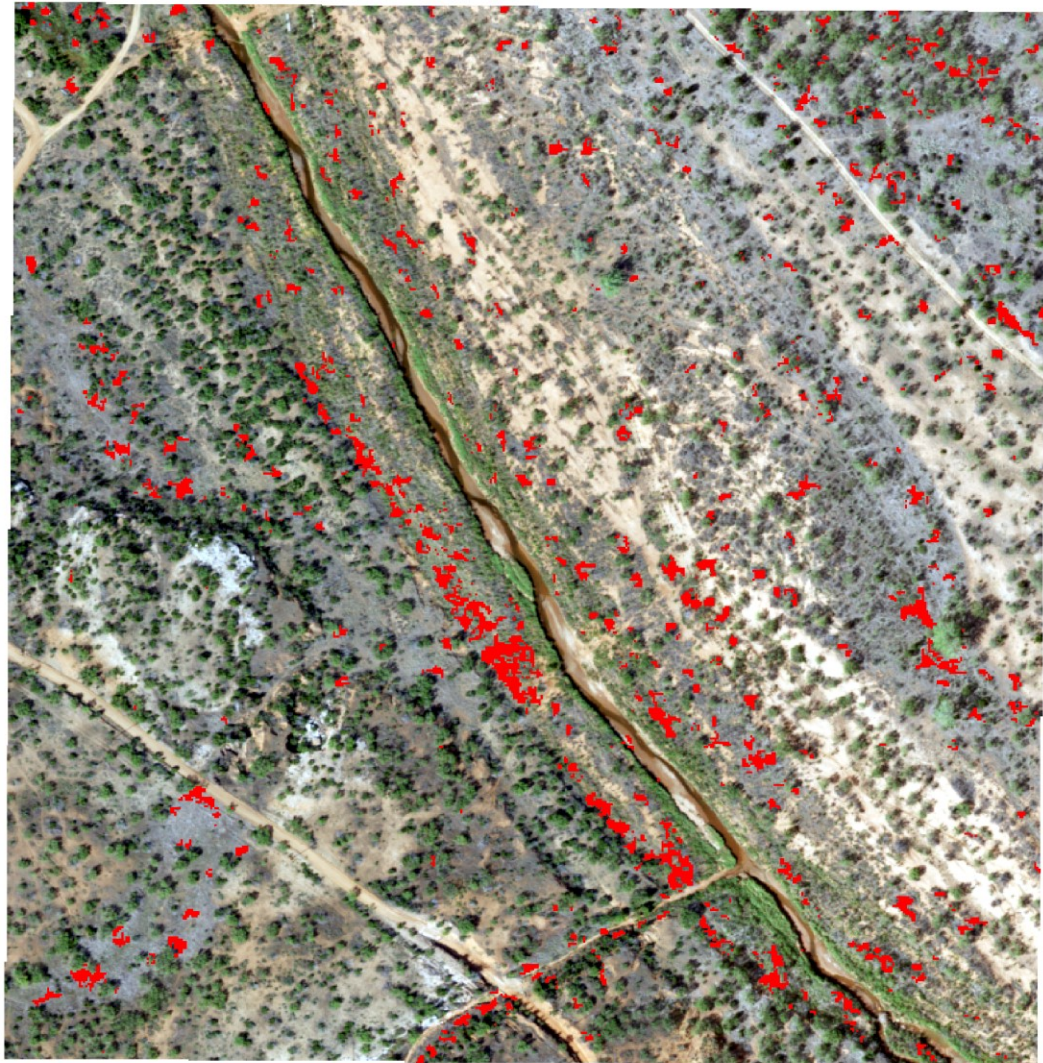
Unchanged Saltcedar



Figure 15. Change detection of unchanged saltcedar for NFD MF 2



## Double Mountain Fork 0 Change Detection



0 0.05 0.1 0.2 Kilometers

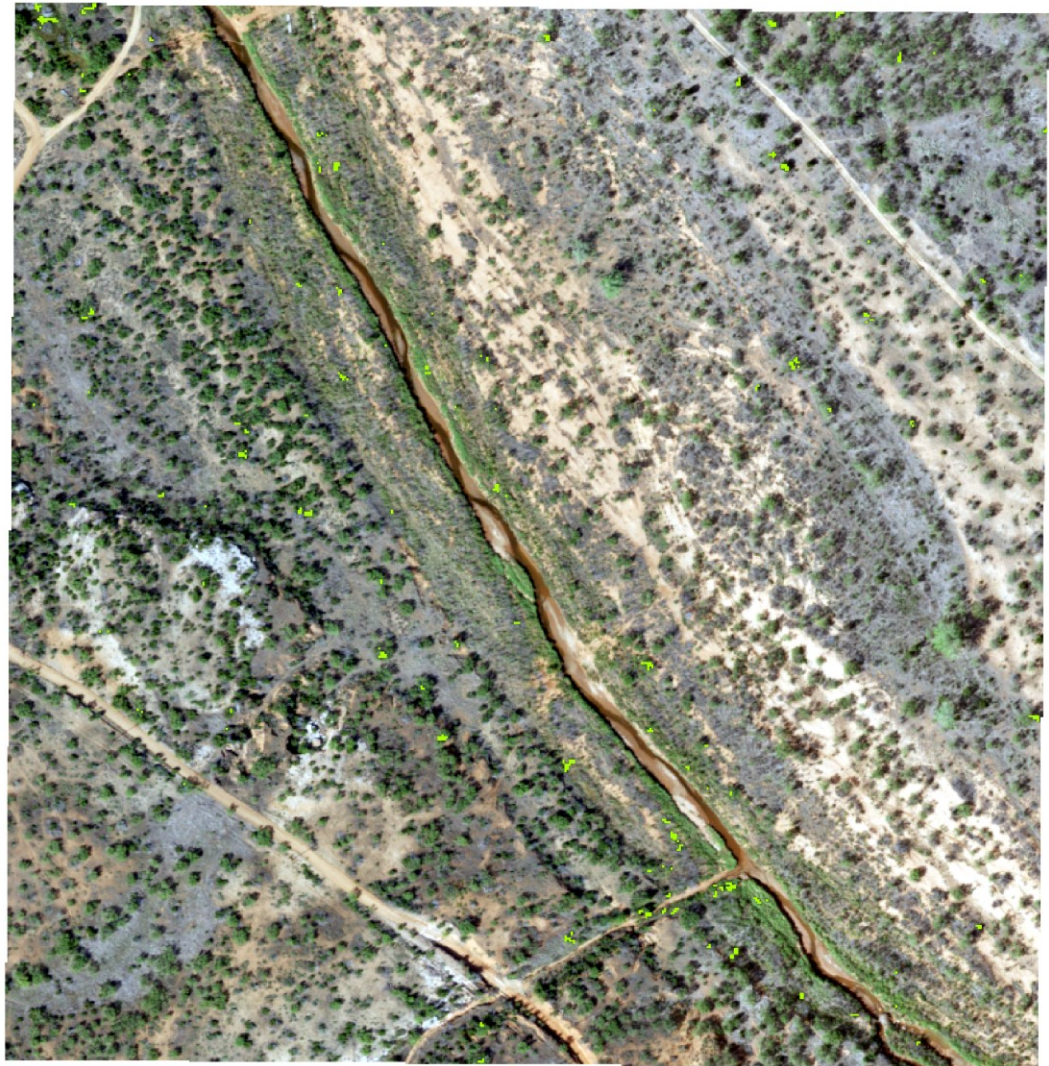
 Healthy Saltcedar to Unhealthy Saltcedar



Figure 16. Change detection of saltcedar for DMF 0



### Double Mountain Fork 0 Change Detection




 Unchanged Saltcedar



Figure 17. Change detection of unchanged saltcedar for DMF 0

### North Fork Double Mountain Fork 1 Floodplain Change Detection



0 0.05 0.1 0.2 Kilometers


 Healthy Saltcedar to Unhealthy Saltcedar



Figure 18. Change detection of saltcedar for NFD MF 1 floodplain

### North Fork Double Mountain Fork 1 Floodplain Change Detection



0 0.05 0.1 0.2 Kilometers


 Unchanged Saltcedar



Figure 19. Change detection of unchanged saltcedar for NFD MF 1 floodplain

## V. DISCUSSION

### NAIP Imagery

Although NAIP imagery provides high spatial resolution, there is low spectral resolution. This lack of spectral resolution created limitations in class creation and classification. Due to this poor resolution, separability between spectrally similar classes such as unhealthy saltcedar and barren or non-vegetated was difficult. These classes were often misclassified throughout all sites and image dates. Spatial resolution of images also influenced classification. In the context of the vegetation, there were many species whose individuals were smaller than one meter. This size issue created situations where one pixel is demonstrating a vegetated spectral response, however, since many of the surrounding pixels were of different classes and larger, the adjacent area would be classified as that of the larger object. Changes in the spatial resolution between image years from 1 m to 60 cm needed to be addressed in the classified images. Resampling the 2020 image to the resolution of the 2012 image was needed to ensure that the change detection was conducted on two images with similar spatial resolution. As some classes returned low accuracies, this study supports the future implementation of higher resolution imagery to identify and classify some vegetation species that would have been omitted or underrepresented.

Temporally, this study might have produced different results if quality images were available for times where saltcedar was in bloom. Their distinct pink and purple flowers would have created both a RGB and NDVI signature that could be useful in better identifying saltcedar. Leaf color changes during autumn and early winter could

also be beneficial to future studies. This approach was taken by Everitt and DeLoach (1990), Groeneveld and Watson (2008), and Diao and Wang (2016), all with varying degrees of success.

During the initial data preprocessing, it was a goal to mitigate the atmosphere's interference with reflectance to create a less denuded product. However, it was found that obtaining Top-of-Atmosphere DN's would not be possible due to the extensive requirement of metadata that was not available. It was decided not to attempt to obtain ToA values.

### **Field Data Collection**

Field vegetation data was collected in May and June of 2022. Data collection occurred within the two-year span between image products, and so the discrepancy of timing between the newest available image and field data collection must be noted when examining the results of this study. The vegetation points were collected on a handheld GPS unit. Descriptions of these points were taken in a field notebook to aid in vegetation identification during the analysis. Many of the points were successfully used in identifying different vegetation covers, and the points whose descriptions greatly differ from what is seen in the NAIP imagery were not used. As the GPS unit had an average error distance of 1.8 m, it was necessary to scrutinize the image and the segmentation to ensure proper identification. As I was not present at these sites in 2012 and 2020, my observations on riparian vegetation come two years after the most recent NAIP image. Due to this, my observations in-situ cannot be definite of the conditions that were present during the time of imaging. This river system experienced few high-magnitude events,

and when they occur their effect on the landscape is preserved until the next event. These changes can occur quickly and can alter the floodplain significantly. It will require multiple years of successional observations to truly explain the rates of change in these floodplains.

### **Image Classification**

Due to the low spectral resolution of NAIP imagery, it was necessary to implement the use of NDVI and texture measures to produce an enhanced image for segmentation and classification. Implementing texture measures in high spatial resolution imagery can yield increased land cover classification accuracy (Franklin et al., 1990). Texture measures provide an enhanced difference between potential land cover classes and aide in image segmentation.

In addition to discrete classes in the classification, it is also important to understand the role of transitional zones in land cover types. In the field, it is evident that many times there is not a defined beginning and ending to land cover types. Instead, they transition into different vegetation types at differing rates. These transitions are difficult to analyze as deciding their class designations for training segment creation and accuracy assessment can become subjective. There is no clear partition between many of these transition zones. Due to this, there were many instances where a pixel contained two or more land cover types but had to be grouped into one discrete class. Many misclassifications were made along these transition zones. Using imagery with greater spatial and spectral resolutions can help to mitigate issues brought on by the mixed pixel issue.



## **Accuracy Assessment**

Due to the low spectral resolution and difficulty identifying smaller vegetation types, I anticipated misclassifications and moderate accuracies. All Kappa values were approximate to the desired 0.61 Kappa coefficient, showing a substantial agreement. Kappa coefficients should be viewed as support to the results, as several studies have established some of the shortcomings of Kappa. Pontius and Millones (2011) examined the role of Kappa and outlined how it is often a metric that serves little purpose in the realm of image classification. However, as this value is seen in countless analyses, it was also included in this study.

In multiple images, the percentages of certain classes remained very small. Coupled with stratified random sampling, accuracy assessment points of small classes amounted to 10 samples of each small class. This influenced the wide ranges of accuracy for those classes. If able in future analyses, it should be a goal to create a large sample size of those classes to help create a more robust summarization of mentioned classes.

In the case of NFDMF 1 and NFDM 1 floodplain, the stratified floodplain overall accuracy for 2012 decreased from 76.30% to 73.59%, yet for 2020, accuracies improved from 66.65% to 77.91% between NFDMF 1 and NFDMF 1 floodplain, respectively. In addition, Kappa values improved in both images. Image stratification led to overall increased accuracies and Kappa values.

## **Change Detection**

In all three detections, healthy saltcedar coverage decreased, and unhealthy saltcedar increased. This change detection suggests that the management efforts of

TPWD have been effective in the treatment of saltcedar in the UBR. During the creation of training segments, it was important to identify areas of dense saltcedar coverage in 2012 as they would be used as a reference to the 2020 images to help identify unhealthy saltcedar. There were many areas in all images where there were large and dense stands of saltcedar in 2012 that became unhealthy saltcedar in 2020. For example, in NFD MF 1 2012, a large and dense stand of many saltcedars could be seen towards the top of the image. In the 2020 image, dead saltcedar occupied the same region. It was much easier to identify large areas of change, but it proved difficult to find and classify moderately dense or single stands of saltcedar without many other saltcedar in the vicinity. Using a higher spatial or spectral resolution image could prove useful in identifying single stands of trees that would lead to higher accuracies and a better overall classification.

In partitioning the image between the original clipped image and the floodplain stratification for NFD MF 1, a larger increase in pixels that transitioned from healthy to unhealthy saltcedar occurred. This shows that focusing on the floodplain can yield a more precise and accurate change detection, as opposed to incorporating image elements not associated with the floodplains. Stratification should be applied to all sites in future analyses to provide more robust demonstration of its potential for improved classification accuracies and change detections.

## **Next Steps**

Given additional time for analysis, I would stratify each of the images to provide additional context between overall accuracies. Additionally, the creation of random accuracy assessment points would have proven useful before the completion of field



work. These points would have served as control points for vegetation surveying, providing a more robust and thorough ground truth observation of the vegetation present. As this research advances, there will be new opportunities to expand upon or adjust the techniques used. Due to instrumentation limitations, utilizing technology with higher spatial and spectral resolutions may lead to higher accuracies and better change detections. Along with changes in instrumentation, adopting new approaches for image processing might also be utilized to better detect the presence and change in saltcedar. Structure from Motion (SfM) is a photogrammetric imaging technique for estimating structures in three dimensions from sequences of two-dimensional images. This technical approach provides a high-resolution landform model of the study sites. SfM would be able to capture and display the differences between saltcedar health, as well as differentiating between vegetation types. This higher detailed technique would also allow for the inclusion of additional vegetation types that could not be included in this analysis due to spatial and spectral constraints. Using this technique would produce classifications that are more representative of present vegetation types, while doing so with higher accuracies. Additional adjustments to instrumentation could also include the implementation of LiDAR (Light Detection and Ranging). This is a remote sensing technique that uses light pulses to measure distances and elevations. Along with SfM, these techniques could be used to create a classification that can better distinguish the structure of a healthy saltcedar from an unhealthy saltcedar.

## VI. CONCLUSION

In this research, OBIA analyses were conducted on three sites of TPWD's effort to manage the invasive phreatophyte saltcedar to detect changes in coverage. Imagery was before and after the beginning of management efforts. The analysis used high spatial resolution NAIP imagery where an NDVI layer with texture measures was created and stacked with the original NAIP image. Texture measures included IDM and ENT to create an enhanced segmentation of the image. Supervised classification began with creating training sets and labeling objects. Using a RF classifier, classified images were created. Utilizing in-situ observations and GIS data as references, accuracy assessments were performed and yielded overall accuracies ranging from 68.65% for NFDMP 1 2020, to 79.35% for NFDMP 2 2012. Six of the eight Kappa values exceeded 0.61, which indicates a substantial agreement in accuracy.

Change detections were performed on all classified maps. All four detections resulted in an overall decrease in healthy saltcedar coverage. There were also areas of persistent growth in all detections. Due to some limitations concerning the spectral resolution of the images, there were large ranges of accuracies produced which varied by class. Field observations also agree that there is substantial evidence for the effectiveness of TPWD management efforts.

While this study developed a time series change detection of vegetation, historic images were not used to better comprehend the conditions and trends seen in that river system. Inclusion of these historic images would have also opened an avenue to explore the history of saltcedar invasion and how it has influenced the very composition and

geometry of the NFDMP and DMF since its introduction to the United States.

This work could benefit from additional in-situ observations and more robust field data collection. Additionally, incorporating higher spatial resolution imagery should reveal more accurate and comprehensive results. The work expressed in this thesis along with the various associated works in this region represent only a part of a constantly changing and adjusting river system.

This research contributes a map product that has not been made available for this type of analysis in this specific region. This research focuses on detecting change in the presence of an exotic and invasive species, saltcedar. This work can be used as a benchmark for adopting similar classification methods for arid river systems that have been affected by invasive riparian vegetation. This study successfully implemented the use of OBIA to detect the change in saltcedar coverage in NAIP imagery over an 8-year period in areas that have been the focus of management efforts.

## REFERENCES

- Akashch, O.Z., C. M. Neale, and H. Jayanthi. 2008. Detailed mapping of riparian vegetation in the middle Rio Grande River using high resolution multi-spectral airborne remote sensing. *Journal of Arid Environments* 72 (9): 1734-1744.
- Allan, J. D., and A. S. Flecker. 1993. Biodiversity conservation in running water. *BioScience* 43 (1): 32-43.
- Anderson B. W. A., A. Higgins, R. D. Ohmart. 1977. Avian use of saltcedar communities in the lower Colorado River Valley. In Johnson, R. R., and D. A. Jones (tech. coords.) *Importance, Preservation, and Management of Riparian Habitat, U.S. Forest Service RM-43*: 128-136.
- Auerbach, H. S. 1943. Father Escalante's Journal, with related documents and maps. *Utah Historical Quarterly* 9: 1-142.
- Baum, B. R. 1967. Introduced and naturalized tamarisks in the United States and Canada (Tamaricaceae). *Beileya* 15: 19-25.
- Baum, B. R. 1978. The genus *Tamarix*. Israel Academy of Science and Humanities.
- Bean, D., T. Dudley, and K. Hultine. 2013. Bring on the beetles. The history and impact of tamarisk biological control. In Sher, A., and M. F. Quigley (eds.). *Tamarix: a case study of ecological change in the American West*. Oxford University Press, New York: 377-403.
- Blackburn, W. H., R. W. Knight and J. L. Schuster. 1982. Saltcedar influence on sedimentation in the Brazos River. *Journal of Soil and Water Conservation* 37 (5): 298-301.
- Blaschke, T. 2010. Object based image analysis for remote sensing. *ISPRS Journal of Photogrammetry and Remote Sensing* 65 (1): 2-16.
- Blaschke, T., G. J. Hay, M. Kelly, S. Lang, P. Hoffman, E. Addnik, R. Q. Feitosa, F. van der Meer, H. van der Werff, F. van Coillie, and D. Tiede. 2014. Geographic object-based image analysis-towards a new paradigm. *ISPRS Journal of Photogrammetry and remote sensing* 87: 180-191.
- Boer, W. J., and D. J. Schmidly. 1977. Terrestrial mammals of the riparian corridor in Big Bend National Park. In Johnson, R. R., and D. A. Jones, (tech. coords). *Importance, Preservation, and Management of Riparian Habitat*. U.S. Department of Agriculture GTR RM-43: 212-217.

- Bowser, C. W. 1958. Introduction and spread of the undesirable tamarisks in the Pacific southwestern section of the United States and comments concerning the plants' influence on the indigenous vegetation. In Symposium on Phreatophytes 12-17.
- Breiman, L., J. H. Friedman, R.A. Olshen, and C. J. Stone. 1984. Classification and regression trees (1<sup>st</sup> ed.). New York, NY: Routledge.
- Brotherson, J. D., J. G. Carman, and L. A. Szyska. 1984. Stem-diameter age relationships of *Tamarix ramosissima* in central Utah. *Rangeland Ecology & Management / Journal of Range Management Archives* 37 (4): 362-364.
- Brotherson, J. D., and V. Winkel. 1986. Habitat relationships of saltcedar (*Tamarix ramosissima*) in central Utah. *Great Basin Naturalist* 46 (3): 535-541.
- Brotherson, J. D., and D. Field. 1987. *Tamarix* impacts of a successful weed. *Rangelands Archives* 9 (3): 110-112.
- Burkham, D. E. 1976. Flow from small watershed adjacent to the study reach of the Gila River Phreatophyte Project, Arizona. U.S. Geological Survey Professional Paper 655-I: 1-18.
- Burnett, C., and T. Blaschke. 2003. A multi-scale segmentation/object relationship modelling methodology for landscape analysis. *Ecological Modelling* 168 (3): 233-249.
- Busby Jr., F. E., and J. L. Schuster, 1973. Woody phreatophytes along the Brazos River and selected tributaries above Possum Kingdom Lake. Texas Water Development Board Report 168: 1-41.
- Busch, D. E., N. L. Ingraham, S. D. Smith. 1992. Water uptake in woody riparian phreatophytes of the southwestern United States: a stable isotope study. *Ecological Applications* 2 (4): 450-459.
- Butler Jr, J. J., G. J. Kluitenberg, D. O. Whittemore, S. P. Loheide II, W. Jin, M. A. Billinger, and X. Zhan. 2007. A field investigation of phreatophyte-induced fluctuations in the water table. *Water Resources Research* 43 (2): 1-12.
- Carman, J. G., and J. D. Brotherson. 1982. Comparisons of sites infested and not infested with saltcedar (*Tamarix pentandra*) and Russian olive (*Elaeagnus angustifolia*). *Weed Science* 30 (4): 360-364.
- Christensen, E. M., 1962. The rate of naturalization of *Tamarix* in Utah. *The American Midland Naturalist* 68 (1): 51-57.

- Cleverly, J. R., S. D. Smith, A. Sala, D. A. Devitt. 1997. Invasive capacity of *Tamarix romosissima* in a Mojave Desert floodplain: the role of drought. *Oecologia* 111 (1): 12-18.
- Cleverly, J. R. 2013. Water use by *Tamarix*. In Sher, A., and M. F. Quigley (eds.). *Tamarix: a case study of ecological change in the American West*: 85-98.
- Cohan, D. R., B. W. Anderson, and R. D. Ohmart. 1978. Avian population responses to saltcedar along the lower Colorado River. *U.S. Forest Service General Technical Report WO-12*: 371-381.
- Cooksey, D., and R. Sheley. 1997. Noxious weed survey and mapping system. *Rangelands* 19 (6): 20-23.
- Cooper, D. J., J. S. Sanderson, D. I. Stannard, and D. P. Groeneveld. 2006. Effects of long-term water table drawdown on evapotranspiration and vegetation in an arid region phreatophyte community. *Journal of Hydrology* 325 (1-4): 21-34.
- Costa, H., G. M. Foody, and D. S. Boyd. 2018. Supervised methods of image segmentation accuracy assessment in land cover mapping. *Remote Sensing of Environment* 205: 338-351.
- Crins, W. J., 1989. The Tamaricaceae in the southeastern United States. *Journal of the Arnold Arboretum* 70 (3): 403-425.
- Crowl, T. A., T. O. Crist, R. R. Parmenter, G. Belovsky, and A. E. Lugo. The spread of invasive species and infectious disease as drivers of ecosystem change. *Frontiers in Ecology and the Environment* 6 (5): 238-246.
- Davenport, D. C., P. E. Martin, and R. M. Hagan. 1982. Evapotranspiration from riparian vegetation: water relations and irrecoverable losses for saltcedar. *Journal of Soil and Water Conservation* 37 (4): 233-236.
- Dean, D. J., M. L. Scott, P. B. Shafroth, and J. C. Schmidt. 2011. Stratigraphic, sedimentologic, and dendrogeomorphic analyses of rapid floodplain formation along the Rio Grande in Big Bend National Park, Texas. *Geological Society of America Bulletin* 123 (9-10): 1908-1925.
- Delay, L., D. M. Finch, S. Brantley, R. Fagurland, M. D. Means, and J. F. Kelly. 1999. Arthropods of native and exotic vegetation and their association with willow flycatchers and Wilson's warblers. In D. M. Finch, J. C. Whitney, J. F. Kelly, and S. R. Loftin. (tech. cords.) *Rio Grande Ecosystems: Linking Land, Water and People RMRS-P-7*: 216-221.

- DeLoach, C. J., R. I. Carruthers, J. E. Lovich, T. L. Dudley, and S. D. Smith. 2000. Ecological interactions in the biological control of saltcedar (*Tamarix spp.*) in the United States: toward a new understanding. *Proceedings of the X International Symposium on Biological Control of Weeds* 2001: 1-66.
- DeLoach, C. J., A. E. Knutson, and P. J. Moran. 2009. Progress on biological control of saltcedar. U.S. Department of Agriculture and Texas AgriLife. [http://www. orangentia.net/SaltcedarPublicReportHandout11-10-09.pdf](http://www.orangentia.net/SaltcedarPublicReportHandout11-10-09.pdf)
- Devitt, D. A., A. Salal, K. A. Mace, and S. D. Smith. The effect of applied water on the water on the water use of saltcedar in a desert riparian environment. *Journal of Hydrology*. 192 (1-4): 233-246.
- Diao, C., and L. Wang. 2016. Incorporating plant phenological trajectory in exotic saltcedar detection with monthly time series of Landsat imagery. *Remote Sensing of the Environment* 182: 60-71.
- Diffenbaugh, N. S., D. L. Swain, and D. Touma. 2015. Anthropogenic warming has increased drought risk in California. *Proceedings of the National Academy of Sciences* 112 (13): 3931-3936.
- DiTomaso, J. M. 1996. Identification, biology, and ecology of saltcedar. In *Proceedings of Saltcedar Management Workshop*. Rancho Mirage, CA. 4-8.
- DiTomaso, J. M. 1998. Identification, biology, and ecology of saltcedar (*Tamarix spp.*) in the Southwestern United States. *Weed Technology* 12 (2): 326-336.
- Doody, T. M., P. L. Nagler, E. P. Glenn, G. W. Moore, K. Morino, K. R. Hutline, and R. G. Benyon. 2011. Potential for water salvage by removal of non-native woody vegetation from dryland river systems. *Hydrological Processes* 25 (26): 4117-4131.
- Dudley, T. L., and B. Collins. Biological invasions in California wetlands: The impacts and control of non-indigenous species in natural areas. *Pacific Institute for Studies in Development, Environment, and Security* 1-38.
- Dudley, T. L., C. J. DeLoach, J. E. Lovich, and R. I. Carruthers. 2000. Saltcedar invasion of western riparian areas: impacts and new prospects of control. In McCabe E., and S. E. Loos, (eds.). *Transactions of the 65th North American wildlife and natural resources conference*. Wildlife Management Institute Washington D. C.: 345-381.
- Duncan, K. W., and K. C. McDaniel. 1998. Saltcedar (*Tamarix spp.*) management with imazapyr. *Weed Technology* 12 (2): 337-344.

- Eakin, M. E., and C. B. Brown. 1939. Silting of reservoirs. *U.S. Department of Agriculture Technical Bulletin* 524: 11-18.
- Echelle, A. A., A. F. Echelle, and L. G. Hill. 1972. Interspecific interactions and limiting factors of abundance and distribution in the Red River pupfish, *Cyprinodon rubrofluviatilis*. *American Midland Naturalist* 88 (1): 1-22.
- Egan, T. B., R. A. Chavez, and B. R. West. 1993. Afton Canyon saltcedar removal first year status report. In Smith, L., and J. Stephenson, (eds.) *Proceedings of the Symposium of Vegetation Management. Hot Desert Rangeland Ecosystems* 1: 1-18.
- Elias, E., A. Rango, R. Smith, C. Maxwell, C. Steele, and K. Havstad. 2016. Climate change, agriculture and water resources in the Southwestern United States. *Journal of Contemporary Water Research & Education* 158 (1): 46-61.
- Engel-Wilson, R. W., and R. D. Ohmart. 1978. Floral and attendant faunal changes on the lower Rio Grande between Fort Quitman and Presidio, Texas. In *Proceedings of the National Symposium Strategies for Protection and Management of Floodplain Wetlands and Other Riparian Ecosystems, General Technical Report GTR-WO-12*. U.S. Forest Service: 139-147.
- ESRI, Inc.. 2022. Website: Train Random Tree Classifier.  
<https://desktop.arcgis.com/en/arcmap/latest/tools/spatial-analyst-toolbox/trainrandom-trees-classifier.htm>.
- ESRI, Inc.. 2022. Website: *Segmentation*.  
<https://pro.arcgis.com/en/proapp/latest/help/analysis/image-analyst/segmentation.htm>.
- Everitt, B. L. 1980. Ecology of saltcedar – a plea for research. *Environmental Geology* 3 (2): 77-84.
- Everitt, J. H., and C. L. DeLoach. 1990. Remote sensing of Chinese tamarisk (*Tamarix chinensis*) and associated vegetation. *Weed Science* 38 (3): 273-278.
- Everitt, B. L., 1998. Chronology of the spread of tamarisk in the central Rio Grande. *Wetlands* 18 (4): 658-668.
- Everitt, J. H., C. Yang, C. J. DeLoach. 2005. Remote sensing of giant reed with QuickBird satellite imagery. *Journal of Aquatic Plant Management* 43: 81-85.
- Fraiser, G. W., and T. N. Johnsen, Jr. 1991. Saltcedar (tamarisk): classification, distribution, ecology, and control. In L. F. James, J. O. Evans, M. H. Ralphs, and R. D. Child, eds. *Noxious Range Weeds*. Boulder, CO: Westview Press 377-386.



- Franklin, S.E., D. R. Peddle, B. A. Wilson, and C. F. Blodgett. 1991. Pixel sampling of Remotely sensed digital imagery. *Computers & Geosciences* 17 (6): 759-775.
- Friederici, P. 1995. The alien saltcedar. *American Forests* 101: 44-47.
- Gatewood, J. S., T. W. Robinson, R. B. Colby, J. D. Hem, and L. C. Halpenny. 1950. Use of Water by Bottomland Vegetation in Lower Stafford Valley, Arizona. U.S. Geological Survey Water Supply Paper 103: 1-224.
- Giardino, J. R., and A. A. Lee. 2011. Rates of channel migration on the Brazos River. Texas Water Development Board Final Report, Contract no. 0904830898: 1-41.
- Glenn, E. P., and P. L. Nagler. 2005. Comparative ecophysiology of *Tamarix ramosissima* and native tress in western U.S. riparian zones. *Journal of Arid Environments* 61 (3): 419-446.
- Goldsmith, F. B., and N. Smart. 1982. Age, spacing and growth rate of *Tamarix* as an indication of lake boundary fluctuation at Sebkhet Kelbia, Tunisia. *Journal of Arid Environments* 5 (1): 43-51.
- Graf, W. L. 1978. Fluvial adjustments to the spread of tamarisk in the Colorado Plateau region. *Geological Society of America Bulletin* 89 (10): 1491-1501.
- Groeneveld, D. P., and R. P. Watson. 2008. Near-infrared discrimination of leafless saltcedar in wintertime Landsat TM. *International Journal of Remote Sensing* 29 (12): 3577-3588.
- Hagemeyer, J., and Y. Waisel. 1990. Phase-shift and memorization of the circadian rhythm of transpiration of *Tamarix aphylla*. *Experientia* 46 (8): 876-877.
- Hamada, Y., D. A. Stow, L. L. Coutler, J. C. Jafolla, and L. W. Hendricks. Detecting Tamarisk species (*Tamarix spp.*) in riparian habitats of Southern California using high spatial resolution hyperspectral imagery. *Remote Sensing of Environment* 109 (2): 237-248.
- Haralick, R. M., and L. G. Shapiro. 1985. Image segmentation techniques. *Computer Visions, Graphics, and Image Processing* 29 (1): 100-132.
- Harwell, G. R., V. G. Stengel, and J. R. Bumgarner. 2016. Simulation of streamflow and the effects of brush management on water yields in the Double Mountain Fork Brazos River watershed, western Texas 1994-2013. U.S. Geological Survey Scientific Investigations Report 2016-5032: 1-50.
- Hay, G. J., D. Marceau, P. Dube, and A. Bouchard. A multiscale framework for landscape analysis: Object-specific analysis and upscaling. *Landscape Ecology* 16 (6): 471-490.

- Hendrickson Jr., K. E. 1952. Website: *Handbook of Texas online: Brazos River*.  
<https://www.tshaonline.org/handbook/entries/brazos-river>.
- Heumann, B. W. 2011. An object-based classification of mangroves using a hybrid decision tree – Support vector machine approach. *Remote Sensing* 3 (11): 2440-2460.
- Horton, J. S. 1964. Notes on the introduction of deciduous *Tamarix*. U.S. Forest Service Research Note RM-16: 1-17.
- Horton, J. S., and C. J. Campbell. 1974. Management of Phreatophyte and Riparian Vegetation for Maximum Multiple Use Values. *U.S. Forest Service Research Paper RM-117*: 1-23.
- Horton, J. S. 1977. The Development and Perpetuation of the Permanent Tamarisk Type in the Phreatophyte Zone of the Southwest. U.S. Rocky Mountain Forest and Range Experiment Station. *U.S. Department of Agriculture Forest Service General Technical Report RM 43*: 124-127.
- Huylenbroeck, L., M. Laslier, S. Dufour, B. Georges, P. Lejeune, and A. Michez. 2020. Using remote sensing to characterize riparian vegetation: A review of available tools and perspectives for managers. *Journal of Environmental Management* 267: 110652.
- Jakle, M. D., and T. A. Gatz. 1985. Herpetofaunal use of four habitats of the Middle Gila River drainage, Arizona. In R. R. Johnson, C. D. Ziebell, D. R. Patton, P. F. Folliot, and R. H. Hamre, (eds.). *Riparian Ecosystems and their Management: Reconciling Conflicting Uses*, 1<sup>st</sup> North American Riparian Conference. U.S. Forest Service Technical Report RM-120: 355-358.
- Ji, W., and L. Wang. 2016. Phenology-guided saltcedar (*Tamarix spp.*) mapping using Landsat TM images in western U.S. *Remote Sensing of the Environment* 173: 29-38.
- Johnson, S. 1987. Can tamarisk be controlled? *Fremontia* 15 (2): 19-20.
- Johnson, D. E. 1999. Surveying, mapping, and monitoring noxious weeds on rangelands. In Sheley, R. L. and J. K. Petroff (eds.), *Biology and Management of Noxious Rangeland Weeds* 19-35.
- Keller, D. L., B. G. Laub, P. Birdsey, and D. J. Dean. 2014. Effects of flooding and tamarisk removal on habitat for sensitive fish species in the San Rafael River, Utah: implications for fish habitat enhancement and future restoration efforts. *Environmental Management* 54 (3): 465-478.

- Kennedy, T. A. 2002. The Causes and Consequences of Plant Invasions. Dissertation. University of Minnesota, St. Paul, MN: 1-160.
- Kerpez, T. A., and N. S. Smith. 1987. Saltcedar Control for Wildlife Habitat Improvement in the Southwestern United States. U. S. Department of the Interior. *Fish and Wildlife Service Resource Publication* 169: 1-16.
- Knutson, A., M. Muegge, T. Robbins, and C. J. DeLoach. 2003. Insects Associated with Saltcedar, *Baccharis* and Willow in West Texas and Their Relative Value as Food for Insectivorous Birds: Preliminary Results. *Proceedings of the Saltcedar and Water Resources in the West*: 16-17.
- Konkle, R. C., 1996. Small Mammal and Herpetofaunal Use of a Saltcedar (*Tamarix chinensis*)-Dominated Riparian Community in Southeastern New Mexico. Thesis. New Mexico State University, Las Cruces, New Mexico: 1-81.
- Laliberte, A. S., A. Rango, K. M. Havstad, J. F. Paris, R. F. Beck, R. McNeely, and A. L. Gonzalez. 2004. Object-oriented image analysis for mapping shrub Encroachment from 1937 to 2003 in southern New Mexico. *Remote Sensing of Environment* 93 (1-2): 198-210.
- Landis, J. R., and G.G. Koch. 1977. The measurement of observer agreement for Categorical data. *Biometrics* 33 (1): 159-174
- Lev-Yadun, S. I., and M. I., Weinstein-Evron. 1994. Late Epipalaeolithic wood remains from el-Wad Cave, Mount Carmel, Israel. *New Phytologist* 127 (2): 391-396.
- Lovich, J. E., and R. C. DeGovenain. 1998. Saltcedar invasion in the desert wetlands of the southwestern United States: ecological and political implications. In Majumdar, S. K. (ed.) *Ecology of Wetlands and Associated Systems*. Pennsylvania Academy of Science: 447-467.
- Lunetta, R. S., J. F. Knight, J. Ediriwickrema, J. G. Lyon, and L. D. Worthy. 2006. Land-cover change detection using multi-temporal MODIS NDVI data. *Remote Sensing of Environment* 105 (2): 142-154.
- Ma, W., Z. Wen, Y. Wu, L. Jiao, M. Gong, Y. Zheng, and L. Liu. 2016. Remote sensing image registration with modified SIFT and enhanced feature matching. *IEEE Geoscience and Remote Sensing Letters* 14 (1): 3-7.
- Macfarlane, W. W., C. M. McGinty, B. G. Laub, and S. J. Gifford. High-resolution riparian vegetation mapping to prioritize conservation and restoration in an impaired desert river. *Restoration Ecology* 25 (3): 333-341.

- Mack, R. N., D. Simberloff, W. M. Lonsdale, H. Evans, M. Clout, and F. A. Bazzaz. 2000. Biotic invasions: Causes, epidemiology, global consequences, and control. *Ecological Applications* 10 (3): 689–710.
- Martinez, M. 1937. Catalogo de Nombres Vulgares y Cientificos de Plantas Mexicanas. *Direccion de Estudios Biologicos* 1-670.
- Mayes, K. B., G. R. Wilde, M. E. McGarrity, B. D. Wolaver, and T. G. Caldwell. 2019. Watershed-scale conservation of native fishes in the Brazos River Basin, Texas. In *American Fisheries Society Symposium* 91: 315-343.
- McDaniel, K. C., and J. P. Taylor. 2003. Aerial spraying and mechanical saltcedar control. In *Proceedings of the saltcedar and water resources in the West symposium*: 100-105.
- McDonald, A. K., B. P. Wilcox, G. W. Moore, C. R. Hart, Z. Sheng, and M. K. Owens. 2015. *Tamarix* transpiration along a semiarid river has negligible impact on water resources. *Water Resources Research* 51 (7): 5117-5127.
- Miller, O. L., A. L. Putnam, J. Alder, M. Miller, D. K. Jones, and D. R. Wise. 2021. Changing climate drives future streamflow declines and challenges in meeting water demand across the southwestern United States. *Journal of Hydrology* X 11: 1-16.
- Milliman, J. D., and R. H. Meade. 1983. World-wide delivery of river sediment to the oceans. *The Journal of Geology* 91 (1): 1-21.
- Mooney, H. A., and J. A. Drake. 1989. Biological invasions: A SCOPE program overview. In J. A. Drake, H. A. Mooney, F. de Castri, R. H. Groves, F. J. Kruer, M. Rejmanék, and M. Williamson (eds.), *Biological Invasions, a Global Perspective*. Chichester, UK: Wiley & Sons, 491–506.
- Mountrakis, G., J. Im, and C. Ogole. 2011. Support vector machine in remote sensing: A Review. *ISPRS Journal of Photogrammetry and Remote Sensing* 66 (3): 247-259.
- Moyle, P. B. 1994. The decline of anadromous fishes in California. *Conservation Biology* 8 (3): 869-870.
- Nagler, P. L., E. P. Glenn, K. Didan, J. Osterberg, F. Jordan, and J. Cunningham. 2008. Wide-area estimates of stand structure and water use of *Tamarix* spp. on the Lower Colorado River: Implications for restoration and water management projects. *Restoration Ecology* 16 (1): 136-145.
- Nagler, P. L., E. P. Glenn, C. S. Jarnevich, and P. B. Shafroth. 2011. Distribution and abundance of saltcedar and Russian olive in the western United States. *Critical Reviews in Plant Sciences*. 30 (6): 508-523.

- Neill, W. M. 1985. Tamarisk. *Fremontia* 12: 22-23.
- Nguyen, U., E. P. Glenn, T. D. Dang, and L. T. H. Pham. 2018. Mapping vegetation in semi-arid riparian regions using random forest and object-based image approach: A case study of the Colorado River Ecosystem, Grand Canyon, Arizona. *Ecological Informatics* 50: 43-50.
- Pal, N. R., and S. K. Pal. 1993. A review on image segmentation techniques. *Pattern Recognition* 26 (9) 1277-1294.
- Parker, I. M., D. Simberloff, W. M. Lonsdale, K. Goodell, M. Wonham, M. H. Williamson, B. von Holle, P. B. Moyle, J. E. Byers, and L. Goldwasser. 1999. Impact: Toward a framework for understanding the ecological effects of invaders. *Biological Invasions* 1 (1): 3-19.
- Perignon, M. C., G. E. Tucker, E. R. Griffin, and J. M. Friedman. 2013. Effects of riparian vegetation on topographic change during a large flood event, Rio Puerco, New Mexico, USA. *Journal of Geophysical Research: Earth Surface* 118 (3) 1193-1209.
- Phillips, J. D. 2007. Perfection and complexity in the lower Brazos River. *Geomorphology* 91 (3-4): 364-377.
- Pimentel, D., R. Zuniga, and D. Morrison. 2005. Update on the environmental and economic costs associated with alien-invasive species in the United States.
- Platt, R. V., and L. Rapoza. 2008. An evaluation of an object-oriented paradigm for land use/land cover classification. *The Professional Geographer* 60 (1): 87-100. *Ecological Economics* 52 (3): 273-288.
- Pontius, R. G., and M. Millones. 2011. Death to Kappa: birth of quantity disagreement and allocation disagreement for accuracy assessment. *International Journal of Remote Sensing* 32 (15): 4407-4429.
- Pu, R., P. Gong, Y. Tian, X. Miao, R. I. Carruthers, and G. L. Anderson. 2008. Using classification and NDVI differencing methods for monitoring sparse vegetation coverage: a case study of saltcedar in Nevada, USA. *International Journal of Remote Sensing* 29 (14): 3987-4011.
- Robinson, T. W. 1965. Introduction, spread, and areal extent of Saltcedar (*Tamarix*) in the western states. *Studies of Evapotranspiration* U.S. Geological Survey Professional paper 491-A 1-8.

- Rowlands, P. G. 1989. History and treatment of the saltcedar problem in Death Valley National Monument. In Kunzmann, M. R., R. R. Johnson, and P. B. Bennett, (tech. coords.) Saltcedar Control in Southwestern U.S. *Proceedings of the Saltcedar Conference, U.S. Department of the Interior Cooperative National Park Resources Study Unit, Special Report 9*: 46-56.
- Sala, A., and S. D. Smith. 1996. Water use by *Tamarix ramosissima* and associated phreatophytes in a Mojave Desert floodplain. *Ecological Applications* 6 (3): 888-898.
- Sanders, T. A., and W. D. Edge. 1998. Breeding bird community composition in relation to riparian vegetation structure in the western United States. *The Journal of Wildlife Management* 62 (2): 1-13.
- Seager, R., M. Ting, C. Li, N. Naik, B. Cook, J. Nakamura, and H. Liu. 2013. Projections of declining surface-water availability for the southwestern United States. *Nature Climate Change* 3 (5): 482-486.
- Shafroth, P. B., J. M. Friedman, and L. S. Ischinger. 1995. Effects of salinity on establishment of *Populus fremontii* (cottonwood) and *Tamarix ramosissima* (saltcedar) in the southwestern United States. *Great Basin Naturalist* 55 (1): 58-65.
- Shafroth, P. B., J. R. Cleverly, T. L. Dudley, J. P. Taylor, C. van Riper, E. P. Weeks, and J. N. Stuart. 2005. Control of Tamarix in the western United States: implications for water salvage, wildlife use, and riparian restoration. *Environmental Management* 35 (5): 231-246.
- Shaner, D. L., and S. L. O'Connor. 1991. The Imidazoline herbicides. CRC Press, Boca Raton, FL: 1-300.
- Skagen, S. K., C. P. Melcher, W. H. Howe, and F. L. Knopf. Comparative use of riparian corridors and oases by migrating birds in southeastern Arizona. *Conservation Biology* 12 (4): 896-909.
- Small, J. F. 1903. Flora of the southeastern United States. *New York Botanical Garden* 1-1370.
- Stevens, L. E. 1985. Invertebrate Herbivore Community Dynamics in *Tamarix chinensis* Loureiro and *Salix exigua* Nuttall in the Grand Canyon, Arizona. Thesis. North Arizona University, Flagstaff, New Mexico: 1-162.
- Stromberg, J. C., M. K. Chew, P. L. Nagler, E. P. Glenn. 2009. Changing perception of change: the role of scientists in *Tamarix* and river management. *Restoration Ecology* 17 (2): 177-186.

- Su, T., and S. Zhang. 2017. Local and global evaluation for remote sensing image segmentation. *ISPRS Journal of Photogrammetry and Remote Sensing* 130: 256-276.
- Szaro, R. C., and S. C. Belfit. 1986. Herpetofaunal use of a desert riparian island and its adjacent scrub habitat. *Journal of Wildlife Management* 50 (4): 1-10.
- Taha, Z. P., and J. B. Anderson. 2008. The influence of valley aggradation and listric normal faulting on styles of river avulsion: a case study of the Brazos River, Texas, USA. *Geomorphology* 95 (3-4): 429-448.
- TPWD. 2018. Management of invasive saltcedar in the upper Brazos watershed: information for landowners. Nonpublished Bulletin.
- TPWD. 2022. Website: *TEAM*.  
<https://tpwd.texas.gov/gis/team/>
- Thompson, C. B. 1958. Importance of phreatophytes in water supply. *Journal of the Irrigation and Drainage Division, Proceedings of the American Society of Civil Engineers* 84 (1): 1-17.
- Thornber, J. J., 1916. Tamarisks for southwestern planting. *Arizona Agricultural Experimentation Station Timely Hints for Farmers* 121: 1-8.
- Tickner, D. P., P. G. Angold, A. M. Gurnell, and J. O. Mountford (2001) Riparian plant invasions: hydrogeomorphological control and ecological impacts. *Progress in Physical Geography* 25 (1): 22-52.
- Turner, H. S. 1974. Quantitative and historical evidence of vegetation changes along the upper Gila River. *Arizona. U.S. Geological Survey Professional Paper* 655-H: 1-20.
- Williams, A. P., E. R. Cook, J. E. Smerdon, B. I. Cook, J. T. Abatzoglou, K. Bolles, S. H. Baek, A. M. Badger, and B. Livneh. 2020. Large contribution from anthropogenic warming to an emerging North American Megadrought. *Science* 368 (6488): 314-318.
- van Hylckama, T. E. A. 1974. Water use by saltcedar as measured by the water budget method. *U.S. Geological Survey Professional Paper* 491-E: 1-29.
- Valente, J., D. Bradsby, K. B. Mayes, C. Loeffler, L. Hamlin, D. Geeslin, K. Horndeski, D. Young, J. Trungle, R. Smith, K. Garmany, and T. Hayes, 2019. Developing a geospatial decision support tool for protecting and restoring environmental flows in Texas rivers and streams. In Dauwalter, D. C., T. W. Birdsong, and G. P. Garrett (eds). *Multispecies and watershed approaches to freshwater fish conservation. American Fisheries Symposium* 91: 253-268.

- Vincent, K. R., J. M. Friedman, and E. M. Griffin. 2009. Erosional consequence of saltcedar control. *Environmental Management* 44 (2): 218-227.
- Wang, L., J. L. Silván-Cárdenas, J. Yang, and A. E. Frazier 2013. Invasive saltcedar (*Tamarisk spp.*) distribution mapping using multiresolution remote sensing imagery. *The Professional Geographer* 65 (1): 1-15.
- Weeks, E. P., H. L. Weaver, G. S. Campbell, and B. D. Tanner. 1987. Water Use by Saltcedar and by Replacement Vegetation in the Pecos River Floodplain between Acme and Artesia, New Mexico. *U.S. Geological Survey Professional Paper* 491-G: 1-31.
- Wilcox, B. P. 2002. Shrub control and streamflow on rangelands: a process based viewpoint. *Journal of Range Management* 55 (4): 318-326.
- Wilcox, B. P., M. K. Owens, W. A. Dugas, D. N. Ueckert, and C. R. Hart. 2006. Shrubs, streamflow, and the paradox of scale. *Hydrological Processes: An International Journal* 20 (15): 3245-3259.
- Yard, H. K., C. van Riper III, B. T. Brown, and M. J. Kearsley. 2004. Diets of insectivorous birds along the Colorado River in Grand Canyon, Arizona. *The Condor* 106 (1): 106-115.
- Yu, Q., P. Gong, N. Clinton, G. Biging, M. Kelly, and D. Schirokauer. 2006. Object-based detailed vegetation classification with airborne high spatial resolution remote sensing imagery. *Photogrammetric Engineering & Remote Sensing* 72 (7): 799-811.
- Zavaleta, E. 2000. The economic value of controlling an invasive shrub. *AMBIO: a Journal of the Human Environment* 29 (8): 462-467.
- Zhou, W., D. Ming, L. Xu, H. Bao, and M. Wang. 2018. Stratified object-oriented image classification based on remote sensing image scene division. *Journal of Spectroscopy* (1): 1-11.